Instituto Tecnológico y de Estudios Superiores de Monterrey

Campus Monterrey

School of Engineering and Sciences

Segmentation of Breast Cancer Masses in Digital Mammograms: A Convolutional Network

A thesis presented by

Erick Michael Cobos Tandazo

Submitted to the
School of Engineering and Sciences
in partial fulfillment of the requirements for the degree of

Master of Science

in

Intelligent Systems

Monterrey, Nuevo León, May, 2016

Instituto Tecnológico y de Estudios Superiores de Monterrey

Campus Monterrey

School of Engineering and Sciences

The committee members, hereby, certify that have read the thesis presented by Erick Michael Cobos Tandazo and that it is fully adequate in scope and quality as a partial requirement for the degree of Master of Science in Intelligent Systems.

Dr. Hugo Terashima Marín
Tecnológico de Monterrey
Principal Advisor

Committee member A's name
Committee member A's institution
Committee Member

Committee member B's name
Committee member B's institution
Committee Member

Graduate Program Director's name
Associate Dean of Graduate Studies
School of Engineering and Sciences

Monterrey, Nuevo León, May, 2016

Declaration of Authorship

I, Erick Michael Cobos Tandazo, declare that this thesis titled, "Segmentation of Breast Cancer Masses in Digital Mammograms: A Convolutional Network" and the work presented in it are my own. I confirm that:

- This work was done wholly or mainly while in candidature for a research degree at this University.
- Where any part of this thesis has previously been submitted for a degree or any other qualification at this University or any other institution, this has been clearly stated.
- Where I have consulted the published work of others, this is always clearly attributed.
- Where I have quoted from the work of others, the source is always given. With the exception of such quotations, this dissertation is entirely my own work.
- I have acknowledged all main sources of help.
- Where the thesis is based on work done by myself jointly with others, I have made clear exactly what was done by others and what I have contributed myself.

Erick Michael Cobos Tandazo
Monterrey, Nuevo León, May, 2016

Dedication

Yet to write

Acknowledgements

Yet to write

Segmentation of Breast Cancer Masses in Digital Mammograms: A Convolutional Network

by

Erick Michael Cobos Tandazo

Abstract

Yet to write

List of Figures

List of Tables

Contents

Chapter 1

Introduction

Discriminating between cancerous and normal tissue in radiographic images of the breast is a complex problem in medical image analysis; in this thesis, we use convolutional networks to tackle it.

Cancer is caused by abnormal cells dividing uncontrollably, forming tumors and eventually invading surrounding tissue. It receives different names based on the part of the body where it originates. Breast cancer, among all cancers, has the highest incidence rate in the United States, an estimated 14.1% of cancer diagnoses in 2015, and the third highest mortality accounting for 6.9% of all cancer-related deaths. Among women, it is the most commonly diagnosed—29% of all cancer cases—and, besides lung cancer, the deadliest—killing 15% of all diagnosed cases [3]. The American Cancer Society recommends women aged 45 or older to get mammograms, images of the breast that show signs of tumor formation, annually or biennially [44]. We consider two types of diagnostic lesions detected on mammograms: clustered microcalcifications, tiny deposits of calcium that could appear around cancerous tissue; and breast masses, more direct signs of the existence of a tumor, although often benign.

Although radiologists are able to identify these lesions with high accuracy, computerized examination may be used to direct their attention to relevant regions, as a second informed opinion or when doctors are unavailable. This motivated the research group to design a computer-aided diagnosis system (CAD) for breast cancer; the present thesis falls under the scope of this project as its first attempt to use deep learning for lesion segmentation.

Traditional CAD systems are pipelines that process the image sequentially using different computer vision techniques; for instance, an standard layout will preprocess the image, identify regions of interest, extract features from the relevant parts and train a classifier on the extracted features. Although many successful systems are built following this pattern, it presents two disadvantages: (1) stages use intricate algorithms and handcrafted features creating an overly complex system that requires many experts to be modified or properly tuned and (2) stages are dependent and relations between them are often obscure: changes in one component affect the performance of others, every component needs to perform well for the system to perform well and every component needs to be improved to improve overall performance.

We use convolutional networks to replace most, if not all, of the stages of traditional image processing. Convolutional networks [20, 31], a natural extension to feedforward neural networks, are statistical learning models that use raw images as input and learn the relevant image features during training. They work well with minimally preprocessed images and

encapsulate segmentation, feature extraction and classification in a single trainable model. Despite some drawbacks, convolutional networks are the state-of-the-art technology for object recognition [51].

Researchers have used small convolutional networks to separate breast masses from normal tissue [52] and individual microcalcifications from noise in the image [34, 21]. A bigger network incorporating newer features such as rectified linear unit activations, pooling, momentum, data augmentation and dropout was trained to identify malignant masses [4]. In these experiments mammograms were enhanced, potential lesions were located and relevant regions were presented to the network for classification. Recently, Dubrovrina et al. [19], segmented different breast tissue using a modern convolutional network. This work relates closely to our own. We train deep convolutional networks end-to-end to identify lesions in digital mammograms.

We aim to learn whether convolutional networks could automatically segment mammographic images, how advantageous it is to use a bigger architecture, more data and tuned hyperparameters and whether we can achieve results similar to those of traditional systems.

In this introductory chapter, we emphasize the importance of the problem in Section 1.1, expand into the problem with traditional image analysis methods in Section 1.2, expose the particular objectives and hypotheses of the thesis in Sections 1.3 and 1.4, offer a brief summary of our methodology in Section 1.5, highlight the particular contributions of this work in Section 1.6 and, lastly, offer an outline of the thesis in Section 1.7.

1.1 Motivation

Breast cancer is the most commonly diagnosed cancer in woman and its death rates are among the highest of any cancer. It is estimated that about 1 in 8 U.S. women will be diagnosed with breast cancer at some point in their lifetime. Early detection is key in reducing the number of deaths; detection in its earlier stage (*in situ*) increases the survival rate to virtually 100% [26].

With current technology, a high quality mammogram is "the most efective way to detect breast cancer early" [41]. Mammograms are used by radiologists to search for early signs of cancer such as tumors or microcalcifications. About 85% of breast cancers can be detected with a screening mammogram [13]; this high sensitivity is the product of the careful examination of experienced radiologists. A computer-aided diagnosis tool (CAD) could automatically detect these abnormalities saving the time and training needed by radiologists and avoiding any human error. Computer based approaches could also be used by radiologists as a help during the screening proccess or as a second informed opinion on a diagnosis.

1.2 Problem Definition

Image segmentation partitions an image into multiple regions, essentially assigning a class to every pixel in the image; for instance, classifying each pixel in a street image as road, building, sky, tree, car, pedestrian, bycicle or background. Lesion segmentation is tasked with separating lesions from normal tissue in medical images. When searching for abnormal findings, radiologists perform lesion segmentation—although implicitly. Traditional CAD systems for

lesion segmentation are based on computer vision methods that are often convoluted and hard-to-adapt [a].

Despite their widespread use and relative success, various limitations should be address to further advance the field:

- Lack of standard preprocessing techniques. Techniques are commonly used but their performance varies.
- Handcrafted features. Image features are chosen beforehand, designed with help of experts and extracted using complex, problem-dependent techniques.
- Expertise needs. Traditional systems require knowledge in many fields such as radiology, oncology, image processing, computer vision and machine learning.
- Pipeline structure. Traditional systems are composed of sequential steps. At each stage, researchers choose among many techniques and adjust their parameters; as achieving an optimal combination of techniques is unlikely, this is both inconvenient and inefficient.
- Low ceiling. Algorithms are already complex and require much work to achieve incremental improvements.
- Complexity. Issues such as non-desired or unknown dependencies between subsystems, difficulty to localize errors and maintainability arise.

In this thesis, we use convolutional networks, a recent development in machine learning, (Sec. 2.3) to remedy some of these problems. In particular, we simplify the system pipeline by using a single end-to-end trainable model that learns the relevant preprocessing and image features from raw data. We can also focus on improving the learning mechanism, both the model and algorithm, rather than working on designing novel image features or improving specific subsystems.

1.3 Objectives

The main goal of this work is to succesfully apply convolutional networks to segment breast cancer lesions in digital mammograms and to compare our results with those obtained by other groups doing similar work. Particularly, there are various subgoals which we expect to achieve as the project advances:

- Obtain and process the mammographic database to make it available for future research on campus.
- Develop software tools to handle the database and train new deep learning models.
- Analyze the performance of convolutional networks reported on the literature.
- Train a modern, fine-tuned convolutional network to perform lesion segmentation.

[a] See [5] for an example.

- Show the viability of convolutional networks for breast cancer detection and diagnosis.
- Generate results that could produce a conference or journal article.
- Use an alternative convolutional network model to improve our results.
- Propose new ideas for future research in the topic.

1.4 Hypothesis

Although a considerable amount of work on breast cancer detection and diagnosis has been done in the institution, this project will be the first approximation to using convolutional networks for efficiently detecting breast cancer. Convolutional networks are widely used for object recognition tasks and have shown very good results [51, 59, 18]. They have a big research community and have become one of the preferred methods for image classification tasks.

Due to the exploratory nature of this work we are uncertain of the results that will be obtained. Nevertheless, we have a well established idea of what to expect. Our hypothesis is that applying convolutional networks to mammographic images will produce similar results to those obtained using more traditional computer vision techniques with less hassle. Additionally, we expect that a simple convolutional network will fail to obtain competitive results; we will need a more refined convolutional network with well fitted hyperparameters. Furthermore, we believe that implementing convolutional networks for this domain will be moderately easy as other groups have already done it (Sec. 2.7) and plenty of software is available.

1.4.1 Research Questions

Some of the questions which will be answered in this work are:

- Can we improve the results reported by other groups using convolutional networks? Is training a convolutional network on mammographic images better than computing numeric features from the mammograms and training a simpler classifier?
- Is deep learning feasible with the resources we have? Is our data and computational power sufficient? Is there any advantage to use GPU acceleration?
- Can we simplify the pipeline for breast cancer detection? Can preprocessing be replaced by more layers on the same convolutional network? Could we use the networks trained for image segmentation to perform detection or diagnosis?
- What are the best parameters for our convolutional networks (number of layers, number of units, kernel sizes, regularization, activation functions, etc)? Is there a big improvement on refining the network and tuning parameters?
- Should we train a convolutional network for each type of breast lesion or could we use a single one with multiple outputs?

- What are the advantages of using a deep versus a shallow convolutional network?
- Could we use a convolutional network trained on a different database (such as the ImageNet database) to obtain features for mammographic images and use these features for classification?
- Are convolutional networks a good option for future research?

1.5 Methodology

We carried out various tasks to achieve the proposed objectives and test our hypotheses. We list them here in order of execution:

1. **Literature review**

   A thorough review of the published work using the databases and resources available in the institution. By the end of this task, a complete theoretical background was obtained and reported. It also helped identify gaps in the literature and refine the scope of the project.

2. **Database processing**

   We looked for a mammographic database adept to our research, asked permission and developped tools to store, preprocess and label the images.

3. **Software review**

   Once we had a clear idea of what experiments will be executed, we found and learned-to-use appropiate software.

4. **Model selection**

   We performed simple experiments to determine the best parameters for the final model. Using these insights and the current literature on convolutional networks, we selected image preprocessing techniques, a network architecture and its features, training and regularization procedures, and evaluation metrics.

5. **Experiments**

   We trained the chosen convolutional network on our mammographic database. We performed crossvalidation to adjust the most important learning parameters and use regularization to avoid possible overfitting. We answered two research questions: is the performance of the convolutional network considerably improved by parameter tuning and, more importantly, is this a good performance?.

6. YET TO WRITE

1.6 Contributions

Yet to write

1.7 Outline of the thesis

This thesis is structured as follows: Chapter 1 introduced the problem and objectives of the thesis, Chapter 2 concisely presents concepts used and gives a thorough literature review, Chapter 3 lists design and implementation details for the final model, Chapter 4 reports experiments and discusses results and Chapter 5 concludes the thesis.

Chapter 2

Background

We offer an introduction to some of the essential concepts needed to understand the rest of this document. We explore basic concepts about classification and evaluation metrics in Section 2.1, introduce artificial neural networks and convolutional networks in Sections 2.2 and 2.3, address image segmentation in Section 2.4, offer advice to deep learning practitioners in Section 2.5, discuss breast cancer in Section 2.6 and review the use of convolutional networks in breast cancer research in Section 2.7.

2.1 Classification

Machine learning is the study of algorithms that build models of a population or function of interest and estimate their parameters from data in order to make predictions or inferences. A machine learning expert knows how to choose the right model for the problem in hand (*model selection*), how to efficiently estimate its parameters from the available data (*learning* or *training phase*) and how to evaluate the trained model (*testing phase*).

Machine learning problems divide into three categories depending on the data used to train the model: *supervised learning*, where we learn a function $f(x)$ using examples labelled with their correct output, for instance, learning to estimate the price of a house given its size and number of bedrooms from a data set of houses with their actual values; *unsupervised learning*, where we look for relationships and structure in unlabelled data, for instance, given a data set of potential customers finding those who are likely to buy a car and *reinforcement learning*, where feedback is received as rewards, for example, learning to play Tetris from a data set of world states, actions and rewards received every time points are earned (when lines dissapear). Supervised learning further divides in regression and classification. If the expected output is numerical, e.g., the price of a house, it is called *regression*, if the expected ouput is categorical, e.g., spam or no spam, it is called *classification*. We focus on classification.

A *classifier* takes as input a vector of *features* $x \in \mathbb{R}^n$ representing a problem instance and produces an *output* $h(x)$ predicting the class y to which that instance belongs, i.e., it models the underlying function $f(x)$ as $h(x)$ (h stands for hypothesis). *Binary classification*, when y can only take two values e.g., cancer/no cancer, is the most common kind of classification and *multiclass classification*, when y can take $K > 2$ different values, can be performed by using K binary classifiers. Some classifiers, such as convolutional networks (Sec. 2.3), output

a *score vector* $h(x) \in \mathbb{R}^K$ where $h(x)_k$ measures the likelihood of x belonging to class k. Every classifier partitions the *feature space*, the n-dimensional space where features exist, into separate *decision regions*, regions of the space that are assigned the same outcome; a *decision boundary* is the hypersurface that partitions the feature space. Classifiers are sometimes classified as *linear* or *nonlinear* according to the nature of the decision boundary they impose on the feature space. Logistic regression, for instance, is a linear classifier while an artificial neural network (with at least one hidden layer) is nonlinear.

The *loss function* $L(\theta)$ of a classifier measures the amount of error the classifier incurs in for a particular choice of parameters θ. This function could be formulated in many ways. A *least-squares loss function* for a binary classifier (such as logistic regression) is presented in Equation 2.1:

$$L(\theta) = \frac{1}{2m} \sum_{i=1}^{m} (h_\theta(x^{(i)}) - y^{(i)})^2 \tag{2.1}$$

where m is the number of training examples, $y \in \{0, 1\}$ is the real class of example x and $h_\theta(x) \in \mathbb{R}$ is the output of the classifier for input x with parameters θ, this represents the probability that x belongs to the positive class 1. We introduce another (rather more complex) loss function in the next section.

A classifier is trained by choosing the parameters θ that minimize its loss function, hence, minimizing the expected error of the classifier on the training set. *Gradient descent* is a method used to estimate these parameters: at the start, it initializes parameters at random and iteratively updates each parameter using the gradient of the loss function until it converges to a minimum. Specifically, at each iteration it performs the update:

$$\theta = \theta - \alpha \nabla L(\theta) \tag{2.2}$$

where α, called the *learning rate*, defines the step size. Gradient descent is guaranteed to converge to a global minimum if the loss function is convex; convexity of the loss function depends on the model $h(x)$.

To select the best model $h(x)$ for a particular problem, or equivalently, to select the best classifier for the problem, we train each model on a subset of the data and evaluate it on a disjoint subset. In the validation set approach the data set is split into a training set (usually 70-90%) and a validation set, each model is trained using the training set, evaluated on the validation set and the best-performing model is selected. *k-fold cross validation*, on the other hand, divides the data set in k disjoint subsets (usually 5 or 10) and uses $k - 1$ subsets to train the model and the remaining subset for evaluation, this process is repeated k times for each model leaving out a different subset each time and the k performance measures are averaged to obtain a final measure for the model. *Model hyperparameters*, settings that modify the underlying model or learning algorithm, are selected in a similar manner.

The model representation $h(x)$ needs to be chosen carefully. If we have an overly *flexible* model, i.e, $h(x)$ is a complex function with many parameters to be learned relative to the size of the training set, the classifier will probably *overfit* the data; this means that parameters are fitted too tight to the training set and pick up small fluctuations and noise causing the classifier to produce almost-perfect results on the training set but perform poorly on unseen examples. The opposite is also true, when $h(x)$ is very simple the classifier lacks the power to model the underlying function of interest and we say that it *underfits* the data.

A popular way to avoid overfitting (and underfitting) is to use a flexible model trained with regularization. *Regularization* modifies the loss function to penalize the complexity of the model, forcing the learning stage to choose parameters that minimize both the training error of the classifier and the complexity of the model. Equation 2.3 shows the least-squares loss function with l_2*-norm regularization*:

$$L(\theta) = \frac{1}{2m}\sum_{i=1}^{m}(h_\theta(x^{(i)}) - y^{(i)})^2 + \frac{\lambda}{2m}||\theta||_2 \tag{2.3}$$

where $||\cdot||_2$ is the euclidean norm of a vector. In addition to reducing training error, minimizing the regularized loss function will shrinken the parameters θ hopefully setting some of them to zero and simplifying $h(x)$. The *regularization strength* λ regulates the tradeoff between less training error and less regularization error. l_1*-norm regularization* or *lasso* is similar to l_2-norm regularization except that it shrinks the l_1-norm of θ instead of the l_2-norm.

We evaluate the performance of a classifier on a separate set of examples, a test set, that should have not been used for training or validation. The standard performance measure in machine learning is classification accuracy; *accuracy* measures the proportion of test set examples correctly classified. Its compliment, *error rate*, measures the proportion of test set examples incorrectly classified. Accuracy, nonetheless, is inappropiate for *unbalanced data sets*, data sets that have many more examples of one class than the other [a]. A classifier that always predicts the predominant class regardless of the input is highly accurate (it is right most of the time) even though it is a bad model for the problem.

In unbalanced data sets, we use metrics based on the confusion matrix of the classifier. A *confusion matrix* summarizes the results of a classifier in the test set (Tab. 2.1). *True*

		Actual class	
		Positive	Negative
Predicted class	Positive	True Positives (TP)	False Positives (FP)
	Negative	False Negatives (FN)	True Negatives (TN)

Table 2.1: Confusion matrix for a binary classifier

positives is the number of positive examples correctly predicted as positive. *False positives* is the number of negative examples incorrectly predicted as positive. True negatives and false negatives are defined similarly. Based on the confusion matrix we can compute some commonly used metrics:

$$Sensitivity \text{ or } Recall = \frac{TP}{TP + FN} \tag{2.4}$$

$$Specificity = \frac{TN}{FP + TN} \tag{2.5}$$

$$Precision = \frac{TP}{TP + FP} \tag{2.6}$$

[a]Cancer data sets are often unbalanced as most examples belong to the negative class (no cancer) than the positive class (cancer)

Sensitivity and specificity are preferred to present results in medical diagnosis meanwhile precision and recall are preferred in machine learning. *Sensitivity* measures the proportion of positive examples predicted as positive and *specificity* measures the proportion of negative examples predicted as negative. *Precision* measures the proportion of examples predicted as positive that are actually positive. A good classifier will have both high sensitivity and high specificity or similarly, high precision and high recall. It is always useful to have a single metric to evaluate classifiers, for example, to choose between two models; we show two commonly used metrics in Equation 2.7 and 2.8.

$$F_1\ score = 2 \times \frac{Precision \times Recall}{Precision + Recall} \tag{2.7}$$

$$G\text{-}mean = \sqrt{Sensitivity \times Specificity} \tag{2.8}$$

The *threshold* of a classifier is the probability at and over which an example is classified as positive. It regulates the trade-off between sensitivity and specificity (or similarly precision and recall): a classifier with a low threshold is prone to classify examples as positive but will potentially produce many false positives thus having high sensitivity but low specificity and viceversa for high thresholds. The *precision-recall curve* of a classifier is a plot of its precision (on the y axis) against its recall (on the x axis) as the threshold varies (Fig. 2.1). The *receiver operating characteristic curve* plots sensitivity (also called true positive rate) against 1-specificity (also called false positive rate) as the threshold varies (Fig. 2.1). The *area under the precision-recall curve* PRAUC and the *area under the receiver operating characteristic curve* AUC summarize the performance of the classifier over all possible thresholds and are used for model selection; they range from 0 to 1 with higher being better. As with previous metrics, AUC is preferred for medical diagnosis while PRAUC is mostly used in machine learning.

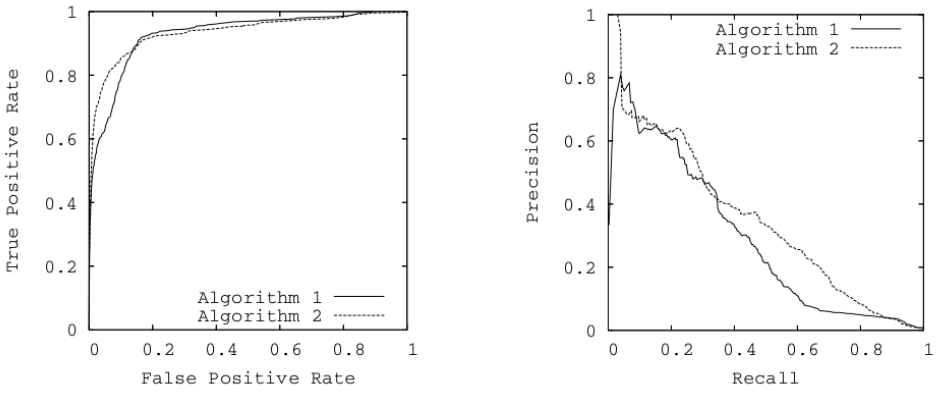

Figure 2.1: A sample receiver operating characteristic curve (left) and precision-recall curve (right). Each algorithm is evaluated on different thresholds and the points produced are used to obtain the curves. Image courtesy of [17]

For unbalanced data sets, "using the classifiers produced by standard machine learning algorithms without adjusting the output threshold may well be a critical mistake" [48]. It is

preferable to use metrics that consider all possible thresholds (AUC or PRAUC) or simpler metrics (F_1 score or G-mean) with a threshold obtained via a validation set. The metric used for model selection influences its characteristics and behaviour, hence, it should be chosen carefully: we favor the use of PRAUC over AUC as well as F_1 score over G-mean because they concentrate in the positive class (cancer) which is harder to predict and more interesting. Furthermore, PRAUC has been shown to have better properties than AUC in unbalanced data sets [17]. In general, we present results for all these metrics.

Finally, we point out that this section is a compendium of basic concepts in machine learning and leaves aside many subtleties of practical machine learning. Notation and content is mostly based on materials from Stanford's Machine Learning course [43].

2.2 Artificial Neural Networks

Artificial neural networks or simply *neural networks* are one of the most popular nonlinear classifiers used today. They were inspired by the way biological neurons integrate information from their dendrites and relay it to neighboring neurons [37, 63, 49] but evolved to specialize in nonlinear modelling at the expense of biological accuracy [50].

Multilayer feedforward neural networks are composed of L layers of *neurons*, units of computation, connected to every unit in the previous and next layer (except for the first and last layer). The first layer, called the *input layer*, has $s^{(1)} = n$ units and receives the feature vector $x \in \mathbb{R}^n$ while the last layer or *output layer* has $s^{(L)} = K$ units corresponding to the K possible classes. Every other layer is called a *hidden layer* (Fig. 2.2). The neural network receives an input $x \in \mathbb{R}^n$, processes it layer by layer and outputs a vector $h_\Theta(x) \in \mathbb{R}^K$, where $h_\Theta(x)_k$ is the predicted (unnormalized log) probability that x belongs to class k. Each unit performs a computation on input from units in the previous layer and transmits the result to units in the next layer through their connections. Furthermore, every connection has a *weight* w that is to be learned in the training phase, i.e, the weights are the parameters Θ of the model. A neural network is *shallow* or *deep* according to its number of layers or *depth* [b].

A unit computes a function of the form:

$$a_i^{(l)} = g\left(\sum_{j=0}^{s^{(l-1)}} \Theta_{ij}^{(l-1)} a_j^{(l-1)}\right) \text{ for } l = 2, \ldots, L-1 \text{ and } i = 1, \ldots, s^{(l)} \tag{2.9}$$

where $a_i^{(l)}$ is called the *activation* or output of unit i in layer l; $g(\cdot)$ is an *activation function* (defined below); $s^{(l)}$ is the number of units in layer l; $a_0^{(u)} = 1$, for all $u = 1, \ldots, L-1$ (defined below); $a_v^{(1)} = x_v$ for all $v = 1, \ldots, n$ i.e., the activation of the input layer is the input x; $a_i^{(L)} = \sum_{j=0}^{s^{(L-1)}} \Theta_{ij}^{(L-1)} a_j^{(L-1)}$ for all $i = 1, \ldots, s^{(L)}$ i.e., $g(\cdot)$ is omitted in the output layer and $\Theta^{(l)} \in \mathbb{R}^{s^{l+1} \times s^l}$ is the matrix of weights connecting layer l to $l+1$. Equation 2.9 may seem convoluted but it simply defines the activation of a unit as the weighted linear combination of the activations of units in the previous layer passed through a function $g(\cdot)$.

[b] Researchers disagree over when a neural network becomes deep [53]. We consider networks with two or more hidden layers to be deep.

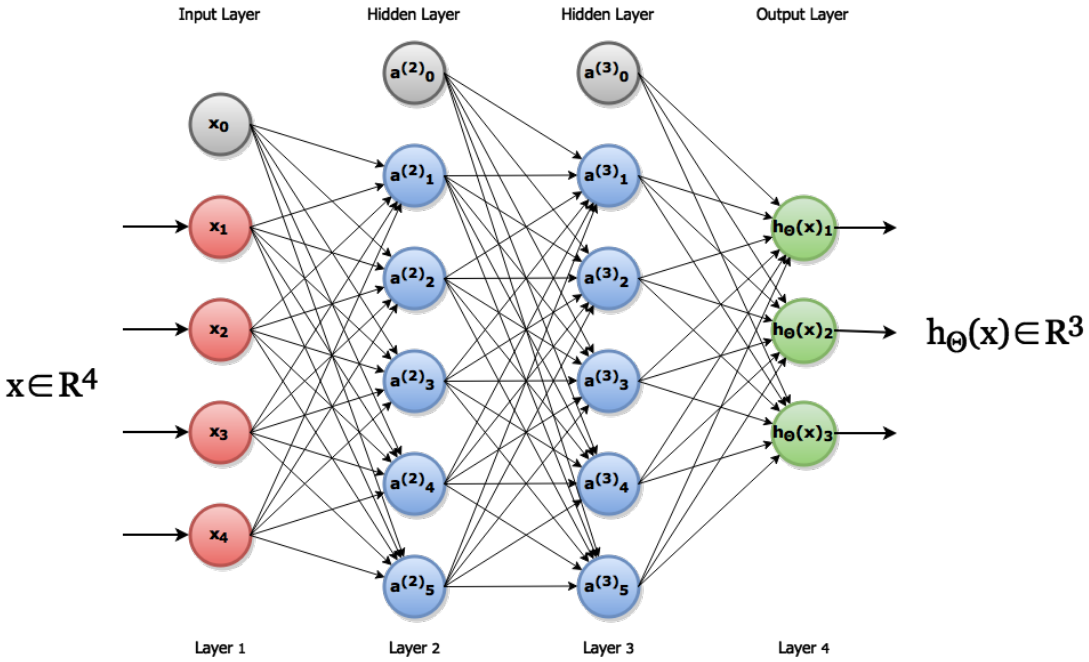

Figure 2.2: A small neural network: input layer with 4 units (red), two hidden layers of 5 units (blue) and output layer of 3 units (green). Bias units appear in gray. It approximates a function $h_\Theta(x) : \mathbb{R}^4 \to \mathbb{R}^3$, i.e., it classifies an input vector $x \in \mathbb{R}^4$ into 3 possible classes.

Each layer (except for the output layer) includes a unit that always outputs activation 1 ($a_0^{(1)} = 1$, $a_0^{(2)} = 1$, etc). These *bias units* allow us to learn a constant parameter Θ_{i0} to account for each unit's inclination or disinclination to activate. Bias units are included in the vectors $a^{(l)}$, hence, the sumation in Equation 2.9 starts at 0 instead of 1.

The activation function $g(\cdot)$ is usually a *rectified linear unit* or *ReLU*:

$$g(z) = \max(0, z) \tag{2.10}$$

This nonlinear function and its derivative ($1_{z>0}$) are computed easily and, unlike sigmoid or tanh activation functions, are inmune to vanishing and exploding gradients. Besides, it greatly accelerates convergence of gradient descent [30] and is currently the recommended activation function for deep neural networks [28].

The vector of activations in the output layer $a^{(L)} \in \mathbb{R}^{s^{(L)}}$, called a *score vector*, equals the predicted (unnormalized log) probabilities $h_\Theta(x) \in \mathbb{R}^K$ so that the class with the highest score in $h_\Theta(x)$ is our prediction for example x. We can exponentiate each of these values and normalize them to obtain a probability distribution over the possible classes K ($p(x) \in [0..1]^K$); this improves interpretability and preserves original predictions.

Every unit produces a nonlinear activation $g(z)$ that is received by units in the next layer, linearly recombined with the activation of other units and passed again through the nonlinear function $g(z)$; these operations repeat until the processed input reaches the output layer. As a result, the network computes a function $h_\Theta(x)$ that is highly nonlinear on the original input x. This explains why neural networks are able to model complex functions and why increasing the number of layers increases its expressive power. It may be insightful to think of each unit

as a feature detector: in the first hidden layer, units learn to detect simple features of the input, in the second hidden layer, units activate when a distinct combination of the simple features is found and so on. Thus, the network learns to recognize the most relevant features of the input and as the number of units increases, it learns ever more complex features.

The *softmax* loss function for a multiclass neural network classifier is defined as:

$$L(\Theta) = -\frac{1}{m}\sum_{i=1}^{m}\log\left(\frac{e^{h_\Theta(x^{(i)})_{y^{(i)}}}}{\sum_{j=1}^{K} e^{h_\Theta(x^{(i)})_j}}\right) \tag{2.11}$$

where m is the number of examples in the training set, $h_\Theta(x)$ is the score vector, K is the number of classes and $(x^{(i)}, y^{(i)})$ is the i^{th} example. $L(\Theta)$ is differentiable with respect to Θ but non-convex, nonetheless, gradient descent usually converges to a good estimate of Θ [43]. *Error backpropagation* [33, 62], an algorithm to calculate the derivatives of the loss function with respect to Θ, computes error terms in the output layer and backpropagates them layer by layer using the chain rule of calculus.

Because many parameters need to be estimated, deep neural networks are susceptible to overfitting. The simplest approach to overcome this is using regularization. Regularization for neural networks is done by performing gradient descent on the regularized loss function presented in Equation 2.12

$$L(\Theta) = -\frac{1}{m}\sum_{i=1}^{m}\log\left(\frac{e^{h_\Theta(x^{(i)})_{y^{(i)}}}}{\sum_{j=1}^{K} e^{h_\Theta(x^{(i)})_j}}\right) + \frac{\lambda}{2m}\sum_{l=1}^{L-1}\sum_{i=1}^{s^{(l)}}\sum_{j=1}^{s^{(l+1)}}\left(\Theta_{ij}^{(l)}\right)^2 \tag{2.12}$$

Dropout [58] is another popular method to prevent overfitting. Each training iteration, dropout samples a different network architecture from the original network and updates only a subset of the values in Θ; a unit (and its connections) is retained with some probability p, usually 0.5, and gradient descent works on this sampled network (Fig. 2.3). During testing all units are active but their activations are scaled by p to match their expected output ($pa_i^{(l)} + (1-p)0$). This is interpreted as training many models (with shared weights) and averaging their results at test time.

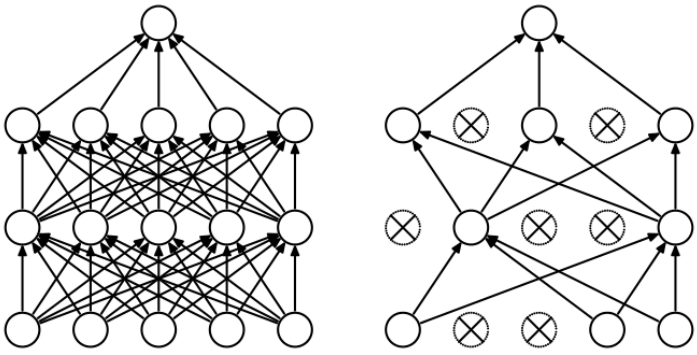

(a) Standard neural network (b) After applying dropout

Figure 2.3: Dropout applied to a simple neural network. Crossed units are dropped. Image courtesy of [58].

2.3 Convolutional Networks

Convolutional networks are inspired by models of the visual cortex [20] but, like regular neural networks, favor practical performance over biological accuracy. Modern convolutional networks were introduced in 1998: LeCun et al. used them to successfully recognize handwritten digits from the MNIST data set [31]. Recently, Krizhevsky et al. achieved state-of-the-art performance on the ImageNet Large-Scale Visual Recognition Challenge [30], an image classification and object localization challenge with 1000 categories [51]. Thanks to recent developments, convolutional networks have become one of the most popular methods for image classification and the driving force behind deep learning.

Due to the number of parameters that would need to be learned, classifying images with regular neural networks is unfeasible; for instance, a small 100×100 grayscale image amounts to 10 000 units in the input layer—a 10 000-dimensional input vector—, therefore, a unit in the second layer would need to learn 10 000 parameters and a simple two-layer network with 100 units in its second layer would have 1 000 000 parameters. Besides, even if data and time requirements were unrestrictive, a regular neural network would destroy the original structure of the image hindering learning. Convolutional networks take advantage of the 2-dimensional structure of images to reduce the number of parameters and facilitate learning.

Layers in a convolutional network are *sparsely connected*, i.e., a unit connects only to a small subset of the units in the previous layer, and *locally connected*, i.e., a unit connects to other units considering their position in the original image. Convolutional networks force *weight sharing* between units in the same layer, i.e., different units share the same parameters. Lastly, *pooling* subsamples the image reducing the spatial dimensions and adding invariance to local translations. All these features arise from the definition of convolutional networks, which we discuss below.

Each layer in a convolutional network is a set of *feature maps*, 2-dimensional grids of unit activations ($\mathbb{R}^{h \times w}$), arranged into a 3-dimensional *volume* ($\mathbb{R}^{h \times w \times d}$). The input layer is a volume ($\mathbb{R}^{h \times w \times c}$) that holds the input image of size $w \times h$ with c color channels. The output layer is a volume of size $R^{1 \times 1 \times K}$ where feature maps are single activations ($R^{1 \times 1}$) representing the final score for each k class. The network receives an image x as an input volume that is transformed layer by layer into new volumes (whose dimensions may differ from the previous ones) until it reaches the output layer of size $h_\Theta(x) = R^{1 \times 1 \times K}$(Fig. 2.4).

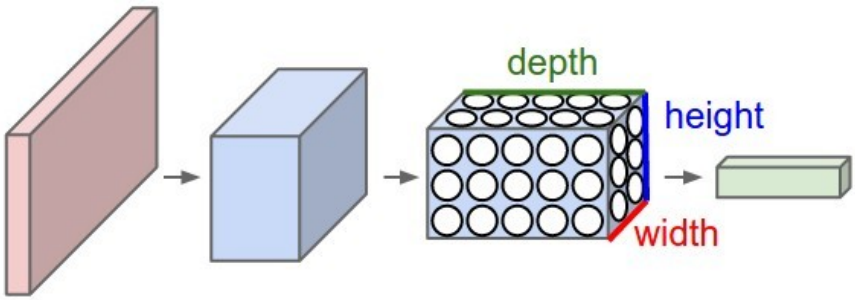

Figure 2.4: Transformations computed by a convolutional network. Input layer is shown in pink, hidden layers are shown in blue and output layer is shown in green. The third layer has 5 feature maps of size 2×3 (width is listed first by convention). Image courtesy of [28].

We buid a convolutional network using four types of layers: convolutional layer, ReLU layer, pooling layer and fully connected layer; all of which compute a differentiable function on its input.

Convolutional layer Convolutional layers are the heart of convolutional networks. They apply filters to the volume in the previous layer; a *filter* is a matrix of weights that has a small spatial size (width and height) but goes across all feature maps of the volume (the third dimension). For instance, a 3×3 filter applied to a volume with 10 feature maps will have 90 parameters ($\mathbb{R}^{3\times3\times10}$) (Fig. 2.5). Feature maps are computed separately and stacked together to form the output volume of the layer. A feature map is obtained by sliding a filter across the spatial dimensions of the previous volume calculating the dot product (a weighted sum) between the filter and the input at each position [c]. All values in a single feature map are computed using the same filter; these filters are the parameters that need to be learned.

We could think of each filter as looking for an specific feature on the input and the feature map as showing its likelihood at each position. If we regard each feature map as a grid of units, we notice that units connect only to a small local subset of units in the previous volume and that all of them share the same weights (Fig. 2.5).

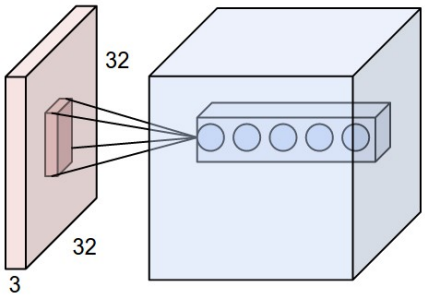

Figure 2.5: Convolutional layer applied to a volume ($\mathbb{R}^{32\times32\times3}$). The resulting volume has five feature maps as shown by the units in the blue volume ($\mathbb{R}^{32\times32\times5}$). Five small filters slide accross the spatial dimensions (32×32) of the volume to produce the feature maps. Image courtesy of [28].

We choose four hyperparameters for this layer: number of feature maps, filter size, stride (the number of places to shift the filter at each step) and amount of padding around the volume; these define the shape of the resulting volume. The number of feature maps depends on the amount of distinct features we wish to learn, the filter size is usually small (3×3 to 9×9), stride is 1 and zero-padding is usually $\lfloor (f_s - 1)/2 \rfloor$ where f_s is the filter size; the last one is needed to preserve the spatial dimensions of the volume in the previous layer.

ReLU layer This layer performs an elementwise ReLU activation function to the volume in the previous layer, i.e., each value z in the volume is passed through the nonlinearity $\max(0, z)$. It outputs a volume with the same dimensions of the previous one and has no parameters to learn. A ReLU layer (or any other activation function) usually follows a convolutional layer so it is sometimes considered part of it; we separate them for clarity.

[c] Each filter also adds a bias term.

Pooling layer The pooling layer subsamples the volume in the previous layer reducing the size of its feature maps but keeping their number. Max pooling slides a fixed-sized windows (normally 2×2) with stride 2 (without overlapping) along each feature map and selects the maximum element on that space. This reduces each feature map dimension by half reducing the total number of activations by 75%, e.g., a 4×4 feature map gets subsampled to a 2×2 feature map where values are the maximum activation in each of the four quadrants of the original feature map. Pooling is applied to each feature map separately. A popular variant of max pooling uses 3×3 windows with stride 2, allowing for overlapping.

Fully connected layer A fully connected layer is a convolutional layer with $w \times h$ filters where w and h are the spatial dimensions of the volume in the previous layer and no zero-padding, i.e., filters cover the entire volume, resulting in feature maps with size 1×1. The output layer of a convolutional network is always fully connected with as many feature maps as possible classes.

The standard convolutional network architecture can be represented textually as:

```
INPUT -> [[CONV -> RELU]*N -> POOL?]*M -> [FC -> RELU]*K -> FC
```

where `*N` indicates that the components are repeated `N` times, `?` indicates an optional component and `N,M,K >= 0`. We use this template to build a large range of models from a linear classifier `INPUT -> FC` (`N,M,K = 0`) to a regular neural network `INPUT -> [FC -> RELU]+ -> FC` (`N,M = 0, K > 0`) to a convolutional network `INPUT -> [[CONV -> RELU]+ -> POOL?]+ -> [FC -> RELU]* -> FC` (`N,M > 0, K >= 0`).

For example, a typical deep convolutional network could be:

```
INPUT -> [[CONV -> RELU]*2 -> POOL]*3 -> [FC -> RELU]*2 -> FC
```

This network receives an input volume (the image), computes two sets of convolution plus ReLUs before pooling and repeats this pattern three times followed by fully connected layers plus ReLUs which are repeated twice and the output layer that reports the final classification scores. Although there is not a standard way of counting the number of layers, we usually ignore ReLU and pooling layers because they lack learnable parameters. Therefore, our network has 10 layers (21 in total), which is a good depth for big data sets. Practical advice on choosing an architecture is offered in Section 2.5.

Figure 2.6 shows a convolutional network with different kinds of layers. The image was obtained in a simulation accesible at `cs231n.stanford.edu`.

Lately, simpler convolutional network architectures have emerged. The All Convolutional Net [57] is a network formed solely by convolutional layers: we replace pooling layers with convolutional layers with the same filter size, stride and number of feature maps; it learns the pooling operation. *Transfer learning* is a related trend where we train a convolutional network on data from a specific domain and later reuse it to extract image features in a different domain or as an initial network to fine-tune with new data.

The loss function for a multiclass convolutional network is similar to that for a regular neural network (Eq. 2.12) except that, in this case, the convolutional network defines the

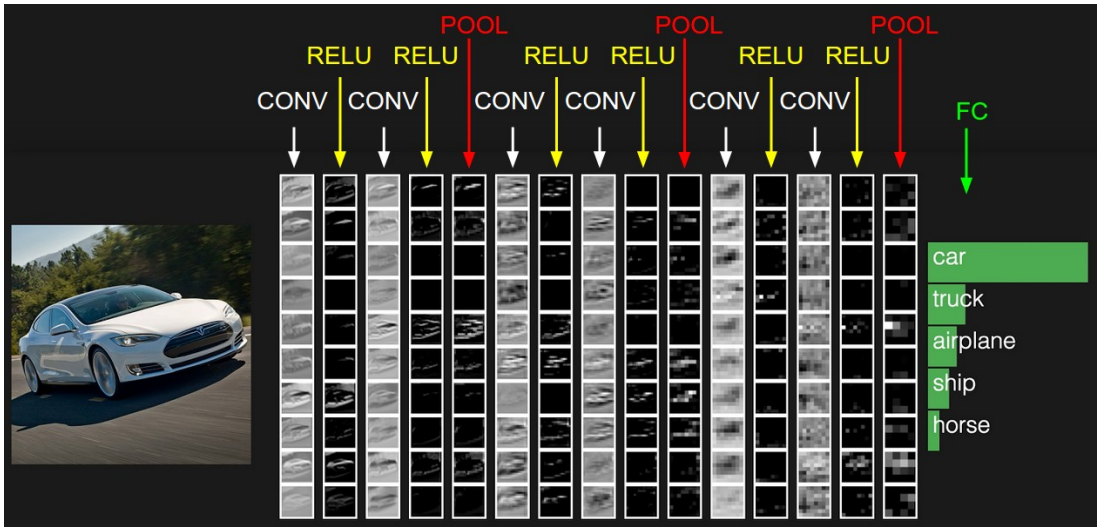

Figure 2.6: Convolutional network with architecture `INPUT -> [[CONV -> RELU]*2 -> POOL]*3 -> FC`. The input image has size 32×32. Each hidden layer uses 10 feature maps (shown as columns). Although the size of feature maps looks constant, each pooling layer reduces its dimensions by half (after the final pooling layer, feature maps have size 4×4). We show final scores for the five most probable classes. Image courtesy of [28].

vector score $h_\Theta(x)$.

$$L(\Theta) = -\frac{1}{m}\sum_{i=1}^{m}\log\left(\frac{e^{h_\Theta(x^{(i)})_{y^{(i)}}}}{\sum_{j=1}^{K} e^{h_\Theta(x^{(i)})_j}}\right) + \frac{\lambda}{2m}\sum_{l=1}^{L-1}\sum_{i=1}^{s^{(l)}}\sum_{j=1}^{s^{(l+1)}}\left(\Theta_{ij}^{(l)}\right)^2 \tag{2.13}$$

This function is differentiable with respect to Θ, thus, we can train the entire network via gradient descent. We calculate the gradient of the loss function with backpropagation.

2.4 Image Segmentation

Image segmentation is the process of labelling each pixel in an image according to the object to which it belongs (Fig 2.7). We can segment an image by training a classifier on small patches, sliding it across bigger images to obtain per-pixel predictions and assigning each pixel to its highest predicted class.

Convolutional networks automatically behave this way when presented with a bigger image than those used for training, albeit, due to subsampling in the pooling layers, they produce a coarse segmentation that needs to be upsampled to match the size of the original image. For instance, a convolutional network trained with 32×32 images and two pooling layers (that reduce the input by a factor of 4) acts as a 32×32 filter with stride 4 in big images, so for a 256×256 image it will produce a 64×64 segmentation [d] that needs to be upsampled by a factor of 4 to recover the original dimensions. To account for the difference in size between the output of the network and the labelled image—the ground truth segmentation—,

[d] Padding the original image by $\lfloor (f_s - 1)/2 \rfloor = 15$ where $f_s = 32$ is the filter size

(a) Original image (b) Segmentation

Figure 2.7: Segmentation of an image with five classes. Image courtesy of [36]

we downsample the labelled image during training or append an upsampling layer at the end of the network [36]; the additional layer computes a differentiable function either fixed such as bilinear interpolation or learned such as a linear mapping. Lastly, the loss function sums the loss over all pixels so the network performs a single gradient update after a segmentation. Convolutional networks transform image segmentation into an end-to-end, learnable task.

To evaluate the model, we evaluate each segmentation using standard metrics (Sec. 2.1) and average over all test images. *Pixel accuracy*, for instance, is the average proportion of correctly classified pixels in an image. Another popular metric, *intersection over union* or *IOU*, is calculated for a single segmentation as $TP/(TP + FP + FN)$ (Tab. 2.1).

If we are interested in a particular class, e.g. object vs. background, we present a single score map showing its probability distribution across every position in the image. We can refine this map using gaussian smoothing, cluster-based thresholding and conditional random fields among other techniques. Finally, we threshold the post-processed map at some specific value to produce a segmentation; the threshold can be chosen using a validation set.

2.5 Practical Deep Learning

In this section we collect guidelines for building as well as efficiently training deep convolutional networks; while they are specific to this thesis, they may prove useful in similar projects. Deep learning is a fast-changing field so these recommendations may soon outdate.

Image preprocessing Convolutional networks handle raw image data, but some level of preprocessing speeds training and improves performance.

- Crop images to contain only the relevant regions, denoise, enhance and resize them to maintain the input size fixed and manageable.
- Zero-center each image feature (the raw pixels) by subtracting its mean across all training images. Optionally, normalize each zero-centered feature to range from $[-1 \dots 1]$ by dividing them by its standard deviation [28].

- Test data should not be used to calculate any statistic used for preprocessing. Furthermore, the same statistics (calculated from training data) should be used to preprocess test data [28].

Convolutional network architecture Designing convolutional networks involves many decisions, we provide recommendations for the architecture and sensible values for related hyperparameters.

- Select a network architecture flexible enough to model the data and manage overfitting rather than a simpler architecture that may be incapable to model the data [43, 30].
- Although, theoretically, neural networks with a single hidden layer are universal approximators provided they have enough units ($\mathcal{O}(2^n)$ where n is the size of the input), practically, deeper architectures produce better results using less units overall. This holds for convolutional networks [8].
- Use at least 8 layers (not counting pooling or ReLU layers) for big data sets, use less layers or transfer learning for small data sets. "You should use as big of a neural network as your computational budget allows, and use other regularization techniques to control overfitting." [28]
- Use 2-3 `CONV -> RELU` pairs before pooling (N above) [28]. Pooling is a destructive operation, placing two convolutional layers together allows them to detect more complex features.
- Use 1-5 `[CONV -> RELU]+ -> POOL` blocks (M above). This hyperparameter regulates the representational power of the architecture. The exact number depends on the complexity of the features in the data and the computational resources available. It also defines how much the volume is subsampled.
- Use less than 3 `FC -> RELU` pairs before the output layer (K above) [28]. The volume that arrives to fully connected layers is already complex, adding many layers only increases the number of parameters and risks overfitting.
- The number of feature maps per convolutional layer controls the number of features detected at that layer—similar to the number of units per layer in a regular neural network. A common pattern is to start with a small amount of feature maps and increase them layer by layer [55].
- The number of feature maps per fully connected layer decreases layer by layer[e]. For instance, for a convolutional network with ten possible classes and two fully connected layers, if the last convolutional layer produces a volume of size $8 \times 8 \times 512$ (8192 units), the first fully connected layer could have size $1 \times 1 \times 2048$ and the second— the output—layer $1 \times 1 \times 10$.

[e]The number of units in a convolutional layer is the number of units in a feature map times the number of feature maps.

- Use 3×3 filters with stride 1 and zero-padding 1 or 5×5 filters with stride 1 and zero-padding 2. This preserves the spatial dimensions of the volume and works better in practice [57]. If the input size is too big, use a bigger filter in the first convolutional layer [28].
- Use 2×2 pooling with stride 2. This pooling and the overlapping version presented in Section 2.3 produce similar results [30].
- Use square input images (width = height) with spatial dimensions divisible by 2. These should be divisible by 2 at least as many times as the number of pooling layers in the network.
- Use number of parameters to measure the complexity of an architecture rather than number of layers or units.

Hyperparameters About setting and searching hyperparameters other than those of the network architecture.

- Use a single sufficiently large validation set (15-30% of data) rather than cross validation [8]. Use cross validation in very small data sets [43].
- Use random search rather than grid search. Random search draws each parameter from a value distribution rather than from a set of predefined values. [10]
- Search for the best combination of hyperparameters rather than each individually.
- Train each combination of hyperparameters for 1-2 epochs to narrow the search space; then, train for more epochs on these ranges [28]. Explore further when the best value for a hyperparameter is found in the limit of the range. [7].
- Partial convergence is sufficient to assess hyperparameters [28].
- Hyperparameters related to the convolutional architecture, e.g., number of layers, number of feature maps and filter sizes are set manually (as explained above) rather than using a validation set.
- Several hyperparameters are set: initial learning rate α, learning rate decay schedule, regularization strength λ, momentum μ, probability of keeping a unit active in dropout p, mini-batch size and type of image preprocessing.
- We could fit all hyperparameters using a validation set but, in practice, this is computationally unfeasible and results in overfitting to the validation data [14].
- Set α, λ and optionally the type of preprocessing using a validation set. Other hyperparameters can be set to a sensible default.
- The learning rate α is "the single most important hyperparameter and one should always make sure that it has been tuned" [7]. It ranges from 10^{-6} to 10^{0}. Use a log scale to draw new values ($\alpha = 10^{unif(-6,0)}$ where $unif(a, b)$ is the continous uniform distribution) [28].

- The regularization strength λ is usually data (and loss function) dependant. It ranges from 10^{-3} to 10^{4}. Search in log scale ($\lambda = 10^{unif(-3,4)}$).
- Halve the learning rate every time the validation error stops improving or choose a fixed number of epochs by observing when the validation error stops decreasing in a similar network [30].
- Use $\mu = 0.9$. If using a validation set try values in $\{0.5, 0.9, 0.95, 0.99\}$ [28].
- Use 0.9-1 probability p of retaining a unit in the input layer, 0.65-0.85 in the first 2-4 convolutional layers and 0.5 in the last convolutional layers and all fully connected layers [58]. Less dropout is used on the first layers because they have less parameters [28].
- Use mini-batch size of 64 or 32. A larger batch size requires more memory and training time. Test performance is unaffected [7].
- Choose among standard preprocessing techniques by (qualitatively) inspecting results on images from the validation set. If none seems superior, fit it along α and λ

Training Convolutional networks have millions of parameters and require careful training. We offer general advice and list some commonly used techniques.

- Shuffle training examples before each epoch to ensure that examples in every mini-batch are sampled independently [7].
- Multiply the number of examples by 25-100 to estimate the maximum number of parameters that could be learned (assuming data augmentation). Groups have learned up to 40M parameters from as little as 60K training examples [18, 57].
- Weight initialization is vital for convergence. Initialize each filter weight as a value from a normal distribution $\mathcal{N}(\mu = 0, \sigma = \sqrt{2/n_{in}})$ where n_{in} is the number of connections to the filter (9 for a 3×3 filter) [24]. In code, `w = randn()*sqrt(2/nIn)` where `randn()` returns values drawn from a standard normal distribution. Initialize biases likewise.
- Use mini-batches rather than the entire training set to compute the gradient of the loss function. Mini-batches allows us to make more updates, more frequently resulting in faster convergence and better test results [7].
- Use Nesterov's Accelerated Gradient (NAG) to update the weights. NAG is a modified version of gradient descent that works better for certain architectures [9]. Stochastic Gradient Descent with Momentum (SGD+Momentum) is also a viable option [28].
- Use dropout as a complement to l_2-norm regularization. Dropout improves results but may slow network convergence [30].
- Store network parameters regularly during training. This allows us to inspect the network at different stages, retrain one or select the one with the best validation error [8].

- Stop training if the validation error has not improved since the last learning rate reduction: gradient descent may not have converged but the validation error will start to increase (overfit) [7].
- If you used test set results to refine a model, shuffle the entire data set and choose a different training and test set to avoid overfitting to the test set [43].

Sanity checks We perform some simple tests to make sure training works properly.

- After weight initialization, run a test on a small set of examples to assert that the network predicts similar scores for every class, the loss function without regularization equals $-\log(1/K)$ and adding regularization increases the loss [28].
- Run a gradient check if backpropagation seems faulty. Gradient checks compare the analytic gradient obtained via backpropagation with a numerical gradient obtained via a finite difference approximation [28].
- Train the network (without regularization) in 10-40 examples to check that the loss function becomes zero. If the network is unable to overfit a tiny subset of data, flexibilize the model. [43].
- During training, the loss function evaluated on training examples decreases monotonically [f]. If not, check for implementation errors, reduce the learning rate or augment momentum [28].
- Monitor the loss function during training to identify underfitting, characterized by high training loss and high validation loss, and overfiting, characterized by low training loss and high validation loss [43].

Image segmentation We usually require to post-process, upsample and threshold the output of a convolutional network to produce a valid segmentation. Given that the network is already trained, using the validation set to choose the best techniques is virtually free.

- For big input images, use smaller mini-batches to avoid overloading the GPU memory [28].
- Set the post-processing technique using the validation set. Conditional random fields are specially effective for refining convolutional network scores [15].
- Use bilinear interpolation for upsampling [15]. If the upsampling factor is greater than 16, use a learnable upsampling layer or skip layers [36].
- Set the segmentation threshold using the validation set; this hyperparameter is equivalent to the threshold used in classification.

[f] Because of momentum and regularization it could increase slightly before decreasing.

Data augmentation We reduce overfitting in image data by applying label-preserving transformations to the original images to generate additional examples. Transformations include rotations, translations, horizontal and vertical reflections, crops, zooms and jittering (adding noise to the colors). The network receives different views of the object and learns invariant features; for instance, if we present images of books at different rotations, we expect it to learn to identify a book on any orientation.

- Exploit invariances you expect in the data set, e.g., galaxies are rotation-invariant because in space there is no up or down [18].
- Be careful to preserve the original label of the image. Applying many transformations may cause the image to lose its meaning.
- Generate the augmented images during training to save storage [30].
- If applying many affine transformations, combine them into a single operation. This is faster and reduces information loss [18].
- Optionally, use data augmentation at test time: present the network with different versions of the image and average its predictions [30].

Unbalanced data In practice, it is common to have very few examples of one class compared to the rest. Managing unbalanced data sets is still an open problem.

- For binary classification with rare positive class, use PRAUC as a performance metric. If the threshold is selected using a validation set, F_1 score is also valid [17].
- For multiclass classification, use the macro-averaged F_1 score, an average of F_1 scores per class, with validated thresholds [45]. A multiclass PRAUC exists but is not used.
- If using an appropiate metric is impractical, divide each predicted class probability by the prior probability of the class and renormalize [12]. This rescales predictions to account for the original imbalance in the class distribution.
- Avoid oversampling, repeating examples from the rare class, and undersampling, discarding examples from the dominant class, because they do not add any information to the data set.
- If rare examples are insufficient for learning, augment them more or balance each minibatch via stratified sampling; the latter is oversampling.

Software We shortly describe four of the most popular packages for deep learning. All have similar capabilities and are available to the public (open-source).

- Tensorflow [1] is a Python/C++ library released by Google that supports automatic differentiation on data flow graphs—neural networks, included—, training on clusters of CPUs and GPUs, graph visualization and easy deployment in multiple platforms. It has been quickly adopted by the deep learning community.

- Caffe [27]: Caffe is a mature deep learning framework developed in C++/CUDA by the Berkeley Vision and Learning Center (BVLC) and community contributors. It offers a Python, Matlab and command line interface; reference models and tutorials; and very fast code with easy GPU activation.
- Theano [11, 6]: Theano is a Python library developed in Python/CUDA at the University of Montreal. It is tightly integrated with NumPy, performs symbolic automatic differentiation and uses the GPU to efficiently evaluate mathematical expressions involving multidimensional arrays.
- Torch7 [16]: Torch is a scientific computing framework developed in C/Lua/CUDA at the IDIAP Research Institute. It offers multidimensional arrays (tensors), automatic differentiation, a command line and Lua interface, GPU support and easy building of complex neural network architectures.

We acknowledge that mammographic data is different from regular image segmentation data: labelling is imperfect, image sizes and ratio change, images are bigger, quality varies, objects of interest are small in relation to the background, data sets are smaller, texture is uniform across the image, among others. Therefore, some of the advice given above may prove counterproductive. Whenever possible, design decisions should be based on data and compiled results.

2.6 Breast Cancer

Cancer is an umbrella term for a group of diseases caused by abnormal cell growth in different parts of the body. The accumulation of extra cells usually forms a mass of tissue called a *tumor*. Tumors can be benign or malignant: *benign tumors* are noncancerous, lack the ability to invade surrounding tissue and will not regrow if removed from the body; malignant or *cancerous tumors* are harmful, can invade nearby organs and tissues (*invasive cancer*), can spread to other parts of the body (*metastasis*) and will sometimes regrow when removed [40].

Breast cancer forms in tissues of the breast. The two most common types of breast cancer are *ductal carcinoma* and *lobular carcinoma*, which start in the breast ducts and lobules, respectively (Fig. 2.8). Breast cancer *incidence rate*, the number of new cases in a specified population during a year, is the highest of any cancer among American women. Its *mortality rate*, the number of deaths during a year, is also one of the highest of any cancer [26].

The *cancer stage* depends on the size of the tumor and whether the cancer cells have spread to neighboring tissue or other parts of the body. It is expressed as a Roman numeral ranging from 0 through IV; stage I cancer is considered *early-stage breast cancer* and stage IV cancer is considered *advanced*. Stage 0 describes non-invasive breast cancers, also known as *carcinoma in situ*. Stage I, II and III describe invasive breast cancer, i.e., cancer has invaded normal, surrounding breast tissue. Stage IV is used to describe metastatic cancer, i.e., it has spread beyond nearby tissue to other organs of the body.

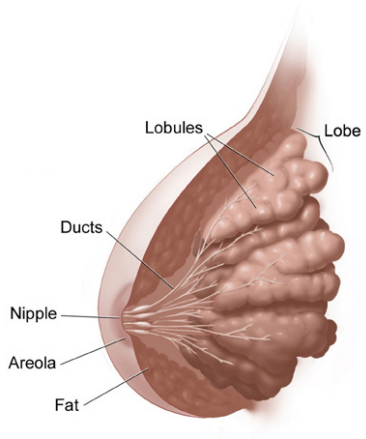

Figure 2.8: Anatomy of the female breast. Image courtesy of [40].

2.6.1 Mammograms

A *mammogram* is an x-ray image of the breast. Radiologists use *screening mammograms* (normally composed of two mammograms of each breast) to check for breast cancer signs on women who lack symptoms of the disease. If an abnormality is found, a *diagnostic mammogram* is ordered; these are detailed x-ray pictures of the suspicious region [41]. A standard mammogram is shown in Figure 2.9.

Figure 2.9: A standard mammogram.

Having a screening mammogram in a regular basis is the most effective method for detecting breast cancer early; around 85% of breast cancers can be detected in a screening mammogram [13]. Nevertheless, screening mammograms have many limitations: a high false positive rate, overtreatment in Stage 0 cancer, false negative results for women with high breast density, radiation exposure and physical and psychological discomfort [41].

Radiologists look primarily for microcalcifications and breast masses. *Microcalcifications* are tiny deposits of calcium in the breast tissue that can be a sign of early breast cancer if found in clusters with irregular layout and shapes (Fig. 2.10). *Breast masses* or breast lumps are a variety of things: fluid-filled cysts, fibric tissues, noncancerous or cancerous tumors, among others. A mass can be a sign of breast cancer if it has an irregular shape and poorly defined margins (Fig. 2.10). Radiologists will also consider the breast density of the patient

when reading a mammogram given that high breast density is linked to a higher risk of breast cancer [2].

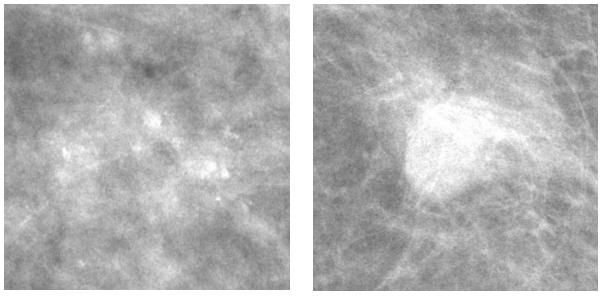

Figure 2.10: Signs of possible breast cancer in a mammogram. Left: A cluster of microcalcifications in an irregular layout. Right: A poorly defined breast mass.

Conventional mammography records mammograms in film; *digital mammography*, on the other hand, converts x-rays into electrical signals and stores images electronically. Digital mammograms offer a clearer picture of the breast and ease manipulation and sharing between health care providers. Although researchers still debate whether they offer an advantage over film mammograms [29, 47, 56], digital mammography has become standard in breast cancer screening. Figure 2.9 is, in fact, a digital mammogram.

Digital tomosynthesis is a new technology that produces three-dimensional x-ray images of the breast and is expected to improve the efficacy of mammograms. Studies comparing the two techniques have not yet been published [41].

Computer-aided detection (CAD) systems assist radiologists during screening signaling suspicious areas and displaying relevant information. Detection or CADe looks for any type of lesion while diagnosis or CADx focuses on malignant lesions. Whether their use improves accuracy has been challenged [32].

2.6.2 Mammographic databases

Researchers use data from previous patients—mammograms, segmentations and clinical features—to train and evaluate their models. *Contrast resolution*, the number of gray values per pixel, and *spatial resolution*, breast area per pixel, dictate the quality of a digital mammogram: 12-bit images ($2^{12} = 4048$ gray values) with pixel size of at most 0.1mm are prefered. Many publicly available databases, including those described below, satisfy these conditions.

The Digital Database for Screening Mammography (DDSM) [25] is the most popular database used for CAD development. It is composed of around 10.5K digitized film mammograms from 2620 patients. Mammograms are either 12-bit or 16-bit images with 0.05 mm spatial resolution. Lesion segmentations are provided along with its type, assesment, subtlety and malignancy.

The BancoWeb database [42] consists of around 1.5K digitized film mammograms from 300 Brazilian patients. Mammograms are 12-bit images with 0.075 or 0.15 mm pixel size. Although few lesions are segmented, this repository may be useful to assess performance in Latin American patients. Its current state is unknown.

Lastly, the Breast Cancer Digital Repository (BCDR-DM) [39, 38] consists of around 1.2K digital mammograms from 237 patients. Mammograms are 8-bit images with 0.07mm spatial resolution. Lesion segmentations are provided as well as their assesment, hand-crafted texture and shape features and relevant clinical data.

This section was written using information from the National Cancer Institute. We recommend to visit its website (`www.cancer.gov`) for further details.

2.7 Convolutional Networks in Breast Cancer Research

Traditional CAD systems for breast cancer are composed of succesive stages: preprocessing and image enhancement, localization of suspicious regions, feature extraction from suspect image patches, feature selection and region classification using machine learning. Tang et al. [60] review the state-of-the-art in CAD systems. We focus on convolutional networks applied to lesion detection and diagnosis in mammographic images.

Overview In 1995, Sahiner et al. [52] used simple convolutional networks to detect masses. Although results were competitive, the research community favored feature-based classifiers, such as regular neural networks, that employed expert knowledge and advanced image techniques. During that time, Lo et al. [34, 35] used convolutional networks to detect individual microcalcifications. This work was continued by Gurcan et al. [23] who selected an optimal architecture to detect individual microcalcifications. The optimized network played a small role in two CADe systems for clustered microcalcifications: one for film mammography [23] and one for digital mammography [22]. Until this point, researchers used few data to train networks (2 to 3 layers, less than 10 thousand parameters) without modern features to classify preselected regions. Recently, Arevalo et al. [4] diagnosed breast masses with a bigger convolutional network (4 layers, 3.4 million parameters) that incorporates many deep learning advances; it outperformed hand-crafted and image-based features. Lastly, Dubrovina et al. [19] trained a convolutional network to perform segmentation of different breast tissues; despite the small network and data set, results were promising. To the best of the author knowledge, this is the only attempt to use supervised convolutional networks for mammographic segmentation [g]. These last studies are the most relevant to this thesis.

In summary, convolutional networks have been used sporadically for breast cancer detection and diagnosis but they have not been used for lesion segmentation or trained with big data sets of digital mammograms.

The following sections expand on the work mentioned above. Architectural details are compiled in Table 2.2

2.7.1 Detection of breast masses

The first attempt to use convolutional networks for breast cancer is reported in ”Detection of masses on mammograms using a convolution neural network” [61]. This four-page article was expanded in [52].

[g] Petersen et al. [46] segmented breast tissue using a convolutional autoencoder.

They used a small convolutional network (2 layers, ∼1K parameters) to detect masses. The data set consisted of 672 manually selected potential masses from 168 digitized mammograms: out of which 168 were positive examples and 504 were dense or fatty tissue. Background reduction was performed using a rather convoluted method. The original images 256×256 (equivalent to 2.56×2.56 cm) were downsampled via non-overlapping average pooling to size 16×16; downsampling to 32×32 pixels was also tried and produced similar results. Data was augmented by using 4 rotations (0°, 90°, 180° and 270°) on each original image and on each horizontally flipped image (8 in total per each training image). The network was trained via batch gradient descent plus momentum and per parameter adaptive learning rate. Two sets of experiments were performed: first, the 16×16 image patches (and their 8 rotations) were used for training producing 0.83 AUC on the best architecture; later, these image patches were complemented with 2 16×16 "texture-images" calculated from the initial image (a $16 \times 16 \times 3$ input volume) producing 0.87 AUC, 0.9 sensitivity and 0.69 specificity with the best network architecture. Authors showed that network architecture was not as important for performance as providing the network with texture information. Texture features give back some of the information lost during downsampling, which explains the improvement. Authors also acknowledge that the network architecture is far from optimal given its simplicity (one convolutional layer with three feature maps) and the incomplete hyperparameter search. A deeper network with bigger input size could produce better results without the need for handcrafted texture features.

2.7.2 Detection of microcalcifications

The first use of convolutional networks to detect microcalcifications is reported in [34]. They performed various experiments on a small convolutional network (3 layers, ∼5.4K parameters). The input size (16×16), number of convolutional layers (2) and kernel size (5×5) were chosen using a validation set, although few options were explored: input sizes of 8, 16 and 32; one and two hidden layers and kernel sizes of 2, 3, 5 and 13. A high sensitivity image technique was used to obtain a set of 2104 image patches (16×16 pixels equivalent to 0.17×0.17 cm) of potential microcalcifications from 68 digitized mammograms; of these, 265 were microcalcifications and 1821 were "false subtle microcalcifications". Prior to training, a wavelet high-pass filter was used to remove the background. Each image was flipped horizontally and 4 rotations for each the original and flipped image were used for training (0°, 90°, 180° and 270°). The network reached 0.89 AUC when identifying individual microcalcifications and 0.97 AUC for clustered microcalcifications—results obtained with a 30-fold cross validation. More than two individual microcalcifications detected on a 1 cm^2 area is considered a cluster detection, the predicted probability for the cluster is the average of the probabilities of all suspect patches inside the 1 cm^2 area [h] Other performance metrics were not explicitly reported. This article showed that deeper networks, background removal and data augmentation improved results. Together with [52], it proved that simple convolutional networks can be used to detect breast cancer lesions.

A convolutional network with a similar architecture (3 layers, ∼4.5K parameters) was presented by the same group in [35]. It detects microcalcifications from 16×16 image patches

[h] This evaluation is not clearly explained in the article or in [35] so our interpretation may be incorrect. This affects the validity of the reported results.

that were pre-selected and preprocessed using the same techniques. For these experiments, nonetheless, they used 38 digitized mammograms and extracted 220 microcalcifications and 1132 negative examples that were randomly divided into a training and test set of roughly equal sizes. The network obtained a 0.9 AUC for individual microcalcifications and 0.97 AUC for clustered microcalcifications (also evaluated as in [34]). It showed that a convolutional network outperforms a regular neural network and a DYSTAL network in detecting clustered microcalcifications when using raw pixels as input features.

Gurcan et al. [23] optimized the filter size and number of feature maps of each convolutional layer of a network used to detect clustered microcalcifications (3 layers, $\sim$7.6K parameters). The convolutional network was part of a CAD system that identifies and enhances the breast area via a bandpass filter, segments potential microcalcifications with adaptive thresholding methods, filters the suspect areas with a rule-based classifier, classifies the remaining image patches with a convolutional network and clusters individual microcalcifications to obtain the detected clustered microcalcifications. The network was trained on 1117 image patches (16×16 pixels equivalent to 0.16×0.16 cm) obtained from 108 digitized mammograms without data augmentation. The best architecture had 14 feature maps on the first convolutional layer with filter size 5×5 and 10 on the second layer with a 7×7 filter. Details about the hyperparameter search or network training are not provided. The CAD reached 84.6% sensitivity at 0.7 false cluster detections per image. The article shows that optimizing the network architecture improves CAD performance significantly; nonetheless, given the small training set and incomplete hyperparameter search results may vary.

Ge et al. [22] tailored the CAD system developed in [23] to digital mammograms. It consists of seven stages: preprocessing via inverted logarithmic transformation, image enhancement via box-rim filter, segmentation of potential microcalcifications via thresholding, classification of individual candidates via rule-based classifier and convolutional network, regional clustering via neighborhood growing, stepwise LDA feature selection and classification via LDA. The convolutional network had the same optimized architecture and was trained on around 500 16×16 image patches obtained from 48 digital mammograms: half of which were microcalcifications. Its threshold was manually set to 0.4. The network reached 0.96 AUC for the detection of individual microcalcification.

These CAD systems were compared in [21]: digital mammograms considerably improved performance. This seems intuitive given that digital mammograms have less noise which allows the system to pick up subtler details without the need for manual enhancement.

2.7.3 Diagnosis of breast masses

Arevalo et al. [4] trained a convolutional network (4 layers, $\sim$3.4M parameters [i]) with modern deep learning techniques to diagnose masses. The data set contained 426 benign and 310 malignant masses obtained from 736 digitized mammograms. Lesions were cropped tightly, resized to 150×150 pixels and augmented (original and flipped images were rotated at 0°, 90°, 180° and 360°). Pixels were normalized globally—subtracting the mean intensity of the 150×150 patch—and locally—subtracting the mean intensity of an 11×11 neighborhood and dividing by its standard deviation. The final architecture was chosen among 25 architectures

[i] They actually learned 4.6 million parameters but many were redundant.

using a validation set. The network extracts image features and forwards them to a separate linear classifier for scoring. This setup competed against linear classifiers trained on HOG features, HGD features, hand-crafted features and features from a convolutional network trained on natural images. The convolutional network trained on mammographic images achieved the best result: 0.86 AUC [j]. Moreover, adding hand-crafted to network-produced features proved ineffective. This work showed that convolutional networks outperform image-based and hand-crafted features in breast cancer diagnosis. They also learned that normalization and additional convolutional layers facilitate learning.

2.7.4 Tissue segmentation

A convolutional network was used in [19] to segment breast tissue into four categories: pectoral muscle, fibroglandular tissue, nipple and general breast tissue. A network was trained on approximately 800 000 overlapping patches (61×61 pixels) cropped from 39 digital mammograms and tested on a single mammogram; this was repeated for every image and results were averaged. Pixels were zero-centered but not further enhanced. The network architecture (6 layers, 34K parameters) was chosen by hand; the network is deep although simple. It was trained using stochastic gradient descent with momentum, learning rate decay, weight decay, dropout and mini-batches of 256 patches. Its output was preprocessed by filling regions and deleting clusters smaller than a predefined threshold. This network reached 0.55 mean IOU. They proved that convolutional networks can perform mammographic image segmentation even with little labelled data. Bigger networks trained with more examples could improve results.

[j] This may be optimistic due to flawed experiment design: examples used to choose the model could belong to the test set.

Table 2.2: Architectures of the convolutional networks used for breast cancer detection and diagnosis.

Article	Goal	Architecture	Volumes	Filters	# Params
[52]	Detect masses	`INPUT -> CONV -> SIGMOID -> FC -> SIGMOID`	$16 \times 16 \times 3$ $7 \times 7 \times 3$ $1 \times 1 \times 1$	10×10 7×7	1047
[34]	Detect individual microcalcifications	`INPUT -> [CONV -> SIGMOID]*2 -> FC -> SIGMOID`	$16 \times 16 \times 1$ $12 \times 12 \times 12$ $8 \times 8 \times 12$ $1 \times 1 \times 2$	5×5 5×5 8×8	5436
[35]	Detect individual microcalcifications	`INPUT -> GAUSSIAN -> [CONV -> SIGMOID]*2 -> FC -> SIGMOID`	$16 \times 16 \times 1$ $12 \times 12 \times 10$ $8 \times 8 \times 10$ $1 \times 1 \times 2$	5×5 5×5 8×8	4530
[23]	Detect individual microcalcifications	`INPUT -> [CONV -> SIGMOID]*2 -> FC -> SIGMOID`	$16 \times 16 \times 1$ $12 \times 12 \times 14$ $6 \times 6 \times 10$ $1 \times 1 \times 1$	5×5 7×7 6×6	7570
[22]	Detect individual microcalcifications	`INPUT -> [CONV -> SIGMOID]*2 -> FC -> SIGMOID`	$16 \times 16 \times 1$ $12 \times 12 \times 14$ $6 \times 6 \times 10$ $1 \times 1 \times 1$	5×5 7×7 6×6	7570
[4]	Diagnose masses	`INPUT -> [CONV -> RELU -> POOL]*2 -> MAXOUT -> SOFTMAX`	$150 \times 150 \times 1$ $140 \times 140 \times 64$ $35 \times 35 \times 64$ $32 \times 32 \times 64$ $8 \times 8 \times 64$ $1 \times 1 \times 400$ $1 \times 1 \times 2$	11×11 5×5 4×4 4×4 8×8 1×1	3.35M

Table 2.2 (continued): Architectures of the different convolutional networks used for breast cancer detection and diagnosis.

Article	**Goal**	**Architecture**	**Volumes**	**Filters**	**# Params**
[19]	Segment tissue	`INPUT -> [CONV -> RELU -> POOL]*3 -> [FC -> RELU]*2 -> SOFTMAX`	$61 \times 61 \times 1$ $55 \times 55 \times 16$ $27 \times 27 \times 16$ $23 \times 23 \times 16$ $11 \times 11 \times 16$ $6 \times 6 \times 16$ $3 \times 3 \times 16$ $1 \times 1 \times 128$ $1 \times 1 \times 16$ $1 \times 1 \times 4$	7×7 3×3 5×5 3×3 5×5 3×3 3×3 1×1 1×1	34324

Chapter 3

Solution Model

In this chapter, we describe our solution, justify design decisions and detail implementation.

3.1 Task definition

We segment digital mammograms into two separate regions: breast mass (benign or malignant) and general tissue. Breast area is previously separated from the background by simple thresholding. In particular, we train a convolutional network to estimate the probability of each pixel belonging to a mass and use these values to generate a valid segmentation.

3.2 Data set

We document the retrieval, enhancement, labelling and augmentation of our data set.

3.2.1 Database

We use the Breast Cancer Digital Repository (BCDR-DM) database. In particular, we use the BDCR-D01 data set, which is composed of patients with at least one breast mass. We have curated it to delete patients with breast implants or other extraneous features ().

We select x digital mammograms from x patients. Theya are 8-bit images with 0.07mm spatial resolution whose size is ta, ta or ta, depending on the size of the placa used to obtain the pictures. Each lesion is segmented and its ... (labels), ..., ..., ... is supplied. Other patient data and image features are supplied but we do not make use of them.

Digital mammograms have higher image quality and lack any marks, stamps or other scanning artifacts present in digitized film mammograms; this allows us to pick up better features and eases segmentation. Although the number of mammograms is small, training on overlapping patches and data augmentation, allows learning.

3.2.2 Data division

70/15/15 is a good split. stratified per patient, this total number of patients in each set and this total number of mammograms (after augmentation) and this total number of lesions.

	Training	Validation	Test	Total
Percentage of data set	70	15	15	100
Number of patients	x	x	x	x
Number of mammograms	x	x	x	x
Number of masses	x	x	x	x
After augmentation	x	x	x	x

Table 3.1: Data set summary

3.2.3 Image dimensions

We decided to hold xbyx cm to hold an entire mass.

We use square image patches because they are common in practice and simplify data augmentation. To define the size we have to consider two aspects: keeping a manageable input size for the network (in pixels) and capturing the entire lesion in the image patch (in mm).

The smallest microcalcification worth considering could be as small as 0.16 mm [35], thus the spatial resolution should be at most 0.16 mm. The standard definition of a cluster of microcalcifications is of 5 or more inside a 1 cm^2 area [54], thus the entire image patch should cover at least a 1 cm^2 area. Using an image patch of 64×64 pixels we cover an image area of 1 cm^2 with a pixel size of 0.156 mm. Mass sizes (length of the long axis) vary from 5 mm to 20 mm [52] [a] There is not really any restriction on spatial resolution other than it being good enough to capture texture information. Again, using an image size of 64×64 pixels we can cover a 4 cm^2 area (2 cm per side) with a spatial resolution of 0.313 mm.

The low spatial resolution (big pixel sizes), however, reduces the quality of the input images. An alternative could be to use 127×127 image patches with 0.079 mm and 0.157 mm pixel sizes for microcalcifications and masses, respectively, aplying a bigger filter on the first convolutional layer, for instance, a 5×5 filter with stride 2 and padding 2. This allows us to have bigger input images with a negligible increase in the number of parameters. Whether the results improve or not is not clear at this point.

Although we use the same input size (either 64×64 or 127×127) for microcalcifications and masses they do not cover the same area in the mammogram. We need to use two different sizes because if we preserve the spatial resolution of microcalcifications, the 1 cm^2 area would not be able to contain the entire mass meanwhile if we use a resolution closer to the one used for masses, small microcalcifications will dissapear and the 4 cm^2 area would have way too much noise compared to the size of the cluster of microcalcifications.

This dictates the spatial dimensions on our input volume in our convolutional network. The amount of pooling in the architecture defines the stride (and thus the amount of overlapping) during training.

We chose a stride of 3 mm. This is midway between a very small stride, say 0.05 mm, which produces many image patches with maximum overlapping and a big stride, say 1 cm, which produces fewer patches with little to no overlapping. We use a rather small stride to have a lesion appear in various image patches (although in a slightly different place in each one) and to produce a good number of patches from the original image (around 1K per

[a] Bigger masses are easily detectable by touch and thus less important for our purposes.

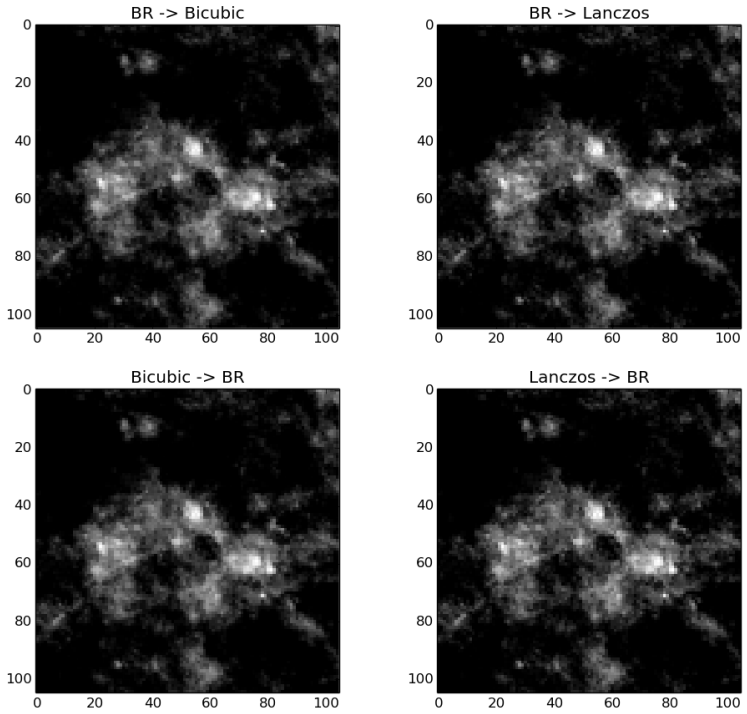

Figure 3.1: Example of different resizing schemes applied to an image with a cluster of microcalcifications. Bicubic and Lanczos inteprolation is used for resizing an original 317 pixel image to 105 pixels before and after enhancement (background reduction plus normalization) as shown by the arrows in the subtitles. Results are virtually undistinguishable.

mammogram). We use no padding.

When sliding the window starting from the upper left corner of the original image it is possible that due to a dimension mismatch pixels in the rightmost and bottom strips do not appear in any image patch, this is not a problem given that the lost strips are very thin (< 3 mm) and they are normally part of the black background.

Resizing We have to resize the images to achieve the desired patch size. There is a couple of decisions to take in this part: the type of interpolation to use and whether image enhancement should be performed before or after resizing. After some experiments neither decisions proved to be very important for the resulting image patches. We choose the Lanczos interpolation recommended for downsizing in the PILLOW Python Image Library. Enhancements are executed on each particular patch before being scaled to their final size. Figure 3.1 shows the effect of using the Bicubic or Lanczos interpolation scheme for resizing both before and after enhancement. Results are similar under all configurations.

3.2.4 Background

We crop the images to the nearest non-zero pixel in x and y.

Mammograms capture images of the breast against a black background which covers a good part of the mammogram. We delete any image patch which is 25% or more black. No important information is lost in this process because the same part of the breast which appears in a deleted patch also appears on other image patches with less black background. A remaining question is how will the trained convolutional network react when presented with an all black input, for example, when slided across the background of a test mammogram. In practice, however, this is not relevant because it is clear that no lesion could occur outside the breast.

An alternative is to preserve all images and let the network learn that black images are negative examples but this seems rather wasteful.

3.2.5 Labels

Once each image patch is obtained we need to assign labels to it. All image patches are initially labelled as negative (or no lesion) and only those where a lesion is present are labelled as positive. There are many ways to define the presence of a lesion in an image: (1) if a percentage of the lesion, say 70% or more, appears in the image, (2) if a percentage of the image is covered by the lesion and (3) if a part of the lesion appears in the middle of the image.

We have chosen the last option to define the presence of a lesion because of three reasons: it is simple to implement, it somehow includes the other methods given that when a lesion appears on the middle of the image patch the rest of it will probably also appear on that patch and finally it encourages the convolutional network to output true only when the lesion appears in the center of the patch but not anywhere else which may give us more granular results when using it on the entire mammogram. The downside is that when a lesion is found on the outside of the image patch (in a corner, for example) it will be labelled as a negative example in the training set and may difficult the learning because even though the lesion is there we are training the network to answer negatively; if this effect actually occurs is not clear. [**?**] uses this method to label its image patches.

Using the first or second option is a viable alternative although they come with their own caveats, for instance, it could be hard to calculate the area of irregular objects or the lesion could be so big that even covering the the entire image patch area it would still not account for 70%.

We will use the type of lession (mass, clustered microcalcifications or normal) and the malignancy (bening, malignant or nothing) to train our networks.

Databases normally offer adittional information such as age of the patient, breast density, family clinical history, assesment of the subtlety and malignancy of the lesion, etc. This information could be used as complementary features before classification or as labels for the network. In this stage we use only the mammograms with the labels stated above (binary classification).

3.2.6 Image enhancement

In theory we want to perform classification on the raw images (without any preprocessing) so we store the raw image patches and their labels as the base training set and perform any image enhancements during training whenever possible. There is a set of simple contrast adjustments that could be applied: normalization assigns 0 to the minimum gray value in the image and 255 (or the maximum available value) to the maximum gray value in the image and stretches the rest of the values linearly, background reduction plus normalization is similar except that all values below a given threshold (the mean of all pixel values in the image) are mapped to zero and the rest is normalized effectively reducing all small variations in the background to black and histogram equalization which tries to distribute the gray values evenly on the histogram of the image. An example of each method is shown in Fig. 3.2.

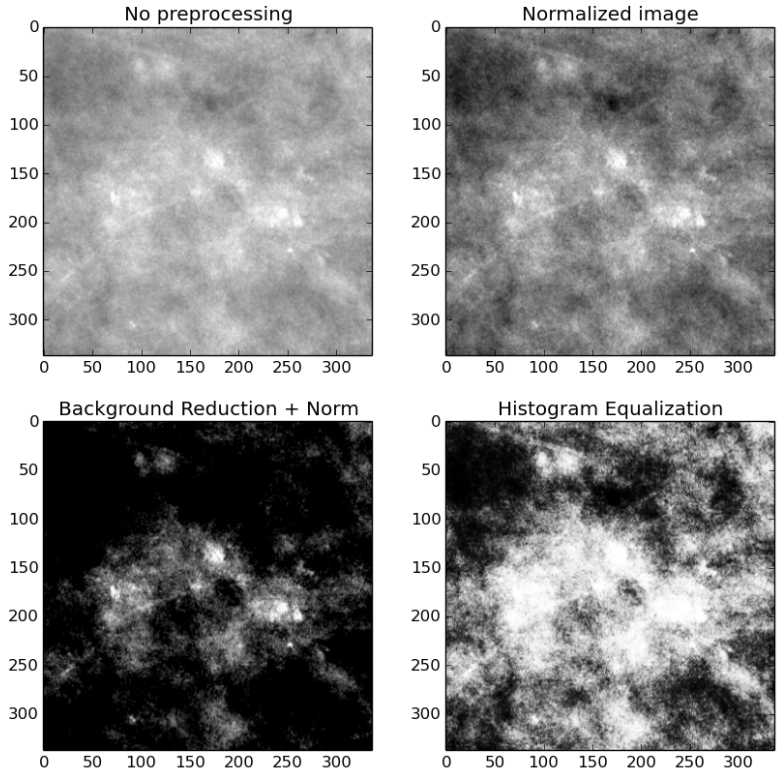

Figure 3.2: Example of simple contrast adjustment techniques applied to an image with a cluster of microcalcifications. Normalization takes the range of gray values and stretchs it up to linearly cover the entire range available. Background reduction assigns 0 to every pixel below the mean of the pixel values and applies normalization. Histogram equalization distributes the gray values more evenly in the histogram of the picture.

We use background reduction plus normalization because it increases the signal to noise ratio, i.e., highlights lesions over normal breast tissue. On the downside, it also highlights dense structures (which could increase false positives) and may destroy important texture information by blending it with the background; using normalization only could produce better

results. Unpreprocessed images seem too noisy and histogram equalization is too destructive for our purposes.

3.2.7 Data augmentation

Rotations and flipping of original big images. the breast and cannals, and nipple may be very different at 90 and 270, flipping an 180 seem fine. Or maybe not. We augment each enhanced image by using 4 rotations (at 0°, 90°, 180° and 270°) of both the original image and a horizontally flipped version of it, thus we increase our data set by a factor of 8. Both rotations and reflections preserve the original label. In principle it is not neccesary to store the augmented images because they can be easily generated during training but if the disk space is not prohibitive explicitly storing them simplifies training.

3.3 Model

3.3.1 Architecture

Using the advice in Section **??** we decided to use a simple network with six convolutional layers and two fully connected layers with the following architecture:

Layer	Filter	Stride	Pad	Volume	Params
INPUT	-	-	-	$127 \times 127 \times 1$	-
CONV -> RELU	5×5	2	2	$64 \times 64 \times 64$	1 625
CONV -> RELU	3×3	1	1	$64 \times 64 \times 64$	36 928
MAXPOOL	2×2	2	0	$32 \times 32 \times 64$	-
CONV -> RELU	3×3	1	1	$32 \times 32 \times 96$	55 392
CONV -> RELU	3×3	1	1	$32 \times 32 \times 96$	83 040
MAXPOOL	2×2	2	0	$16 \times 16 \times 96$	-
CONV -> RELU	3×3	1	1	$16 \times 16 \times 128$	110 720
CONV -> RELU	3×3	1	1	$16 \times 16 \times 128$	147 584
MAXPOOL	2×2	2	0	$8 \times 8 \times 128$	-
FC -> RELU	8×8	-	-	$1 \times 1 \times 512$	4 194 816
FC -> SIGMOID	1×1	-	-	$1 \times 1 \times 1$	513

Table 3.2: Architecture of the network used for experiments. It shows the filter, stride and padding used in each layer as well as the resulting volume and the number of learnable parameters per layer.

The first convolutional layer uses a 5×5 filter with stride 2 (padding 2) to reduce the input spatial size from 127×127 to 64×64. After that all filters are 3×3 with stride 1 (padding 1), which preserves the spatial size and the pooling is 2×2 stride 2 (padding 0) which reduces the spatial size by a half. This architecture has 4.63 million learnable parameters.

In case the input was size 64×64 pixels we could replace use a 3×3 filter with stride 1 in the first convolutional layer and leave everything else unchanged. For an all convolutional

architecture we could replace all pooling layers by a 5×5 filter with stride 2 and use input images of size of 113×113 or 129×129.

3.4 Training

3.4.1 Hardware

Training deep neural networks is computationally intensive and requires equipment with powerful GPUs. We enlist here the resources available for this thesis.

PC	GPU	HD	CPU	RAM	#
Personal	Nvidia NVS 5400M 96 cores, 1GB, 2.1 compatibility, 29 GB/s	57 GB (36 free)	i5-3210M 2.5GHz	4 GB	1
A4-401	Nvidia Quadro K620 384 cores, 2GB, 5.0 compatibility, 29 GB/s	240 GB (230 free)	i5-4570 3.2GHz	8 GB	27

Table 3.3: Available hardware for experiments

3.4.2 Software

We use Caffe [27] to train the networks and Python to develop any other tools (image retrieval and augmentation, model evaluation, figure generation, etc.).

3.4.3 Regularization

Dropout and l2-norm Other options: batch normalization

3.4.4 Hyperparameters

Learning rate decay, dropout p, ...

3.4.5 Implementation details

Python, libraries used,etc.

3.5 Evaluation

3.5.1 Post-processing

Probabilities vs UNcorrected threshold vs Threshold and cluster extent correction vs threshold-free cluster enhancement vs, show different results at different thresholds data is smooth,

uncorrected threshold Present the probabilities of tumor on each pixel. anmd threshold it on a given prob nd delete any clusters less than x. Threshold free cluster enhancement (see module 29 in introduction to fmri) Choose a threshold and delete any clusters less than x...

we could also present a heatmap with the different probabilities in each pixel of the image, for instance on mammograms we could present a grayscale image of whether a lesion is present.

3.5.2 Evaluation

When dividing the data set we make sure *all* image patches obtained from the same patient are assigned to either the training set or test set (not distributed) to avoid any possible overfit to the test set. Given that our data is unbalanced, with far more negative than positive examples, we use PRAUC (see Section **??**) to choose between models for hyperparameter selection and as an overall performance metric. Other metrics are also reported for completeness.

We could also evaluate the network on all augmentations of an image and output the average prediction; in theory, this would give us better results. For simplicity, we do not apply it for model selection.

For detection of lesions on entire mammograms we slide the trained convolutional network across the mammogram computing a per-pixel prediction. The generated heatmap preserves the size of the original mammogram (with some zero-padding) and can be presented side to side to the original mammogram as a CAD system. In case this heatmap is noisy (predictions changes abruptly from pixel to pixel) we could use a median or gaussian filter to smooth it out.

3.5.3 Evaluation metrics

F1-score AUc and those things are calculated only over breast tissue and lessions.

Chapter 4

Mass Segmentation

Task selected. Architecture selected. Hyperparameters selected. results and discussion. We do this as described in chapter 3.

4.1 Results

4.2 Discussion

Chapter 5

Conclusions

5.1 Future Work

Bibliography

[1] ABADI, M., AGARWAL, A., BARHAM, P., BREVDO, E., CHEN, Z., CITRO, C., CORRADO, G. S., DAVIS, A., DEAN, J., DEVIN, M., GHEMAWAT, S., GOODFELLOW, I., HARP, A., IRVING, G., ISARD, M., JIA, Y., JOZEFOWICZ, R., KAISER, L., KUDLUR, M., LEVENBERG, J., MANÉ, D., MONGA, R., MOORE, S., MURRAY, D., OLAH, C., SCHUSTER, M., SHLENS, J., STEINER, B., SUTSKEVER, I., TALWAR, K., TUCKER, P., VANHOUCKE, V., VASUDEVAN, V., VIÉGAS, F., VINYALS, O., WARDEN, P., WATTENBERG, M., WICKE, M., YU, Y., AND ZHENG, X. TensorFlow: Large-scale machine learning on heterogeneous systems, 2015. Software available from `tensorflow.org`.

[2] AMERICAN CANCER SOCIETY. Mammograms and other breast imaging tests. electronic, Atlanta, GA, 2014. Available online on `cancer.org/acs/groups/cid/documents/webcontent/003178-pdf.pdf`.

[3] AMERICAN CANCER SOCIETY. *Cancer Facts & Figures 2015*. American Cancer Society, Atlanta, GA, 2015. Available online on `cancer.org/acs/groups/content/@editorial/documents/document/acspc-044552.pdf`.

[4] AREVALO, J., GONZÁLEZ, F. A., RAMOS-POLLÁN, R., OLIVEIRA, J. L., AND GUEVARA LOPEZ, M. A. Representation learning for mammography mass lesion classification with convolutional neural networks. *Computer Methods and Programs in Biomedicine* (2016).

[5] ASHRAF, A. B., GAVENONIS, S. C., DAYE, D., MIES, C., ROSEN, M. A., AND KONTOS, D. A multichannel markov random field framework for tumor segmentation with an application to classification of gene expression-based breast cancer recurrence risk. *Medical Imaging, IEEE Transactions on 32*, 4 (April 2013), 637–648.

[6] BASTIEN, F., LAMBLIN, P., PASCANU, R., BERGSTRA, J., GOODFELLOW, I. J., BERGERON, A., BOUCHARD, N., AND BENGIO, Y. Theano: new features and speed improvements. Deep Learning and Unsupervised Feature Learning NIPS 2012 Workshop, 2012.

[7] BENGIO, Y. Practical recommendations for gradient-based training of deep architectures. *CoRR abs/1206.5533* (2012). Available online on `http://arxiv.org/abs/1206.5533`.

[8] BENGIO, Y. Deep learning workshop. online, April 2014. Available on youtu.be/JuimBuvEWBg.

[9] BENGIO, Y., BOULANGER-LEWANDOWSKI, N., AND PASCANU, R. Advances in optimizing recurrent networks. *CoRR abs/1212.0901* (2012). Available online on http://arxiv.org/abs/1212.0901.

[10] BERGSTRA, J., AND BENGIO, Y. Random search for hyper-parameter optimization. *J. Machine Learning Research 13*, 1 (February 2012), 281–305.

[11] BERGSTRA, J., BREULEUX, O., BASTIEN, F., LAMBLIN, P., PASCANU, R., DESJARDINS, G., TURIAN, J., WARDE-FARLEY, D., AND BENGIO, Y. Theano: a CPU and GPU math expression compiler. In *Proceedings of the Python for Scientific Computing Conference (SciPy)* (June 2010). Oral Presentation.

[12] BISHOP, C. M. *Neural Networks for Pattern Recognition*. Oxford University Press, Inc., New York, NY, USA, 1995.

[13] BREAST CANCER SURVEILLANCE CONSORTIUM. Performance measures for 1,838,372 screening mammography examinations from 2004 to 2008 by age–based on BCSC data through 2009. electronic, September 2013. Available online on breastscreening.cancer.gov/statistics/performance/screening/2009/perf_age.html.

[14] CAWLEY, G. C., AND TALBOT, N. L. On over-fitting in model selection and subsequent selection bias in performance evaluation. *J. Machine Learning Research 11* (August 2010), 2079–2107.

[15] CHEN, L., PAPANDREOU, G., KOKKINOS, I., MURPHY, K., AND YUILLE, A. L. Semantic image segmentation with deep convolutional nets and fully connected CRFs. *CoRR abs/1412.7062* (2015). Available online on arxiv.org/abs/1412.7062.

[16] COLLOBERT, R., KAVUKCUOGLU, K., AND FARABET, C. Torch7: A matlab-like environment for machine learning. In *BigLearn, NIPS Workshop* (2011).

[17] DAVIS, J., AND GOADRICH, M. The relationship between precision-recall and roc curves. In *Proceedings of the 23rd International Conference on Machine Learning* (New York, NY, USA, 2006), ICML '06, ACM, pp. 233–240.

[18] DIELEMAN, S., WILLETT, K. W., AND DAMBRE, J. Rotation-invariant convolutional neural networks for galaxy morphology prediction. *Monthly Notices of the Royal Astronomical Society* (2015). Available online on arxiv.org/abs/1503.07077.

[19] DUBROVINA, A., KISILEV, P., GINSBURG, B., AND HASHOUL, S. Computational mammography using deep neural networks. In *MICCAI-2015 Proc. Deep Learning in Medical Image Analisys (DLMIA)* (2015).

[20] FUKUSHIMA, K. Neocognitron: A self-organizing neural network model for a mechanism of pattern recognition unaffected by shift in position. *Biological Cybernetics 36* (1980), 193–202. PMID: 7370364.

[21] GE, J., HADJIISKI, L. M., SAHINER, B., WEI, J., HELVIE, M. A., ZHOU, C., AND CHAN, H.-P. Computer-aided detection system for clustered microcalcifications: comparison of performance on full-field digital mammograms and digitized screen-film mammograms. *Physics in Medicine and Biology 52*, 4 (2007), 981.

[22] GE, J., SAHINER, B., HADJIISKI, L. M., CHAN, H.-P., WEI, J., HELVIE, M. A., AND ZHOU, C. Computer aided detection of clusters of microcalcifications on full field digital mammograms. *Medical Physics 33*, 8 (2006), 2975–2988.

[23] GURCAN, M. N., CHAN, H.-P., SAHINER, B., HADJIISKI, L., PETRICK, N., AND HELVIE, M. A. Optimal neural network architecture selection: Improvement in computerized detection of microcalcifications. *Academic Radiology 9*, 4 (2002), 420 – 429.

[24] HE, K., ZHANG, X., REN, S., AND SUN, J. Delving deep into rectifiers: Surpassing human-level performance on imagenet classification. *CoRR abs/1502.01852* (2015). Available online on http://arxiv.org/abs/1502.01852.

[25] HEATH, M., BOWYER, K., KOPANS, D., MOORE, R., AND KEGELMEYER, W. P. The digital database for screening mammography. In *Proceedings of the Fifth International Workshop on Digital Mammography* (2001), M. Yaffe, Ed., Medical Physics Publishing, pp. 212–218.

[26] HOWLADER, N., NOONE, A. M., KRAPCHO, M. F., GARSHELL, J., MILLER, D. A., ALTEKRUSE, S. F., KOSARY, C. L., YU, M., RUHL, J., TATALOVICH, Z., MARIOTTO, A. B., LEWIS, D. R., CHEN, H. S., FEUER, E. J., AND CRONIN, K. A. SEER cancer statistics review, 1975-2011. review, National Cancer Institute, Bethesda, MD, April 2014. Available online on `seer.cancer.gov/csr/1975_2011/`.

[27] JIA, Y., SHELHAMER, E., DONAHUE, J., KARAYEV, S., LONG, J., GIRSHICK, R. B., GUADARRAMA, S., AND DARRELL, T. Caffe: Convolutional architecture for fast feature embedding. *CoRR abs/1408.5093* (2014).

[28] KARPATHY, A. Convolutional neural networks for visual recognition course. online, May 2015. Available on `cs231n.github.io`.

[29] KERLIKOWSKE, K., HUBBARD, R. A., MIGLIORETTI, D. L., GELLER, B. M., YANKASKAS, B. C., LEHMAN, C. D., TAPLIN, S. H., AND SICKLES, E. A. Comparative effectiveness of digital versus film-screen mammography in community practice in the united states: A cohort study. *Annals of Internal Medicine 155*, 8 (2011), 493–502.

[30] KRIZHEVSKY, A., SUTSKEVER, I., AND HINTON, G. E. Imagenet classification with deep convolutional neural networks. In *Advances in Neural Information Processing Systems 25*, F. Pereira, C. Burges, L. Bottou, and K. Weinberger, Eds. Curran Associates, Inc., 2012, pp. 1097–1105.

[31] LECUN, Y., BOTTOU, L., BENGIO, Y., AND HAFFNER, P. Gradient-based learning applied to document recognition. *Proceedings of the IEEE 86*, 11 (November 1998), 2278–2324.

[32] LEHMAN, C. D., WELLMAN, R. D., BUIST, D. S., KERLIKOWSKE, K., TOSTESON, A. N., AND MIGLIORETTI, D. L. Diagnostic accuracy of digital screening mammography with and without computer-aided detection. *JAMA Internal Medicine 175*, 11 (2015), 1828–1837.

[33] LINNAINMAA, S. The representation of the cumulative rounding error of an algorithm as a taylor expansion of the local rounding errors. Master's thesis, University of Helsinki, Helsinki, Finland, 1970.

[34] LO, S.-C. B., CHAN, H.-P., LIN, J.-S., LI, H., FREEDMAN, M. T., AND MUN, S. K. Artificial convolution neural network for medical image pattern recognition. *Neural Networks 8*, 7–8 (1995), 1201 – 1214. Automatic Target Recognition.

[35] LO, S.-C. B., LIN, J.-S. J., FREEDMAN, M. T., AND MUN, S. K. Application of artificial neural networks to medical image pattern recognition: Detection of clustered microcalcifications on mammograms and lung cancer on chest radiographs. *Journal of VLSI signal processing systems for signal, image and video technology 18*, 3 (1998), 263–274.

[36] LONG, J., SHELHAMER, E., AND DARRELL, T. Fully convolutional networks for semantic segmentation. *CVPR* (November 2015). Available on `arxiv.org/abs/1411.4038`.

[37] MCCULLOCH, W. S., AND PITTS, W. A logical calculus of the ideas immanent in nervous activity. *Bulletin of Mathematical Biophysics 5* (1943), 115–133.

[38] MOURA, D. C., AND GUEVARA LÓPEZ, M. A. An evaluation of image descriptors combined with clinical data for breast cancer diagnosis. *International Journal of Computer Assisted Radiology and Surgery 8*, 4 (2013), 561–574.

[39] MOURA, D. C., LÓPEZ GUEVARA, M. A., CUNHA, P., GONZÁLEZ DE POSADA, N., RAMOS-POLLAN, R., RAMOS, I., PINHEIRO LOUREIRO, J., MOREIRA, I. C., FERREIRA ARAÚJO, B. M., AND CARDOSO FERNANDES, T. *Progress in Pattern Recognition, Image Analysis, Computer Vision, and Applications: 18th Iberoamerican Congress, CIARP 2013, Havana, Cuba, November 20-23, 2013, Proceedings, Part I*. Springer Berlin Heidelberg, Berlin, Heidelberg, 2013, ch. Benchmarking Datasets for Breast Cancer Computer-Aided Diagnosis (CADx), pp. 326–333.

[40] NATIONAL CANCER INSTITUTE. What you need to know about breast cancer. electronic, Bethesda, MD, August 2012. Available online on `cancer.gov/publications/patient-education/WYNTK_breast.pdf`.

[41] NATIONAL CANCER INSTITUTE. Mammograms. electronic, March 2014. Available online on `cancer.gov/cancertopics/types/breast/mammograms-fact-sheet`.

[42] NEPOMUCENO MATHEUS, B. R., AND SCHIABEL, H. Online mammographic images database for development and comparison of cad schemes. *Journal of Digital Imaging 24*, 3 (2011), 500–506.

[43] NG, A. Machine learning course. online, December 2014. Available online on coursera.org/course/ml.

[44] OEFFINGER, K. C., FONTHAM, E. T., ETZIONI, R., AND ET AL. Breast cancer screening for women at average risk: 2015 guideline update from the american cancer society. *Journal of the American Medical Association 314*, 15 (2015), 1599–1614.

[45] ÖZGÜR, A., ÖZGÜR, L., AND GÜNGÖR, T. Text categorization with class-based and corpus-based keyword selection. In *Proceedings of the 20th International Conference on Computer and Information Sciences* (Berlin, Heidelberg, 2005), ISCIS'05, Springer-Verlag, pp. 606–615.

[46] PETERSEN, K., NIELSEN, M., DIAO, P., KARSSEMEIJER, N., AND LILLHOLM, M. *Breast Imaging: 12th International Workshop, IWDM 2014, Gifu City, Japan, June 29 – July 2, 2014. Proceedings*. Springer International Publishing, Cham, Switzerland, 2014, ch. Breast Tissue Segmentation and Mammographic Risk Scoring Using Deep Learning, pp. 88–94.

[47] PISANO, E. D., HENDRICK, R., YAFFE, M. J., BAUM, J. K., ACHARYYA, S., CORMACK, J. B., HANNA, L. A., CONANT, E. F., FAJARDO, L. L., BASSETT, L. W., D'ORSI, C. J., JONG, R. A., REBNER, M., TOSTESON, A. N., AND GATSONIS, C. A. Diagnostic accuracy of digital versus film mammography: Exploratory analysis of selected population subgroups in DMIST. *Radiology 246*, 2 (2008), 376–383. PMID: 18227537.

[48] PROVOST, F. Machine learning from imbalanced data sets 101. *Proceedings of the AAAI-2000 Workshop on Imbalanced Data Sets* (2000).

[49] ROSENBLATT, F. *Principles of neurodynamics: perceptrons and the theory of brain mechanisms*. Report (Cornell Aeronautical Laboratory). Spartan Books, 1962.

[50] RUMELHART, D. E., HINTON, G. E., AND WILLIAMS, R. J. Learning internal representations by error propagation. In *Parallel Distributed Processing: Explorations in the Microstructure of Cognition, Vol. 1*, D. E. Rumelhart, J. L. McClelland, and C. PDP Research Group, Eds. MIT Press, Cambridge, MA, 1986, pp. 318–362.

[51] RUSSAKOVSKY, O., DENG, J., SU, H., KRAUSE, J., SATHEESH, S., MA, S., HUANG, Z., KARPATHY, A., KHOSLA, A., BERNSTEIN, M., BERG, A. C., AND FEI-FEI, L. ImageNet Large Scale Visual Recognition Challenge. *International Journal of Computer Vision (IJCV) 115*, 3 (2015), 211–252. Available online on arxiv.org/abs/1409.0575.

[52] SAHINER, B., CHAN, H.-P., PETRICK, N., WEI, D., HELVIE, M. A., ADLER, D. D., AND GOODSITT, M. M. Classification of mass and normal breast tissue: A convolution neural network classifier with spatial domain and texture images. *IEEE Transactions on Medical Imaging 15*, 5 (October 1996), 598–610.

[53] SCHMIDHUBER, J. Deep learning in neural networks: An overview. *Neural Networks 61*, 0 (2015), 85–117.

[54] SICKLES, E., D'ORSI, C., AND BASSETT, L. *ACR BI-RADS Atlas, Breast Imaging Reporting and Data System*, 5th ed. American College of Radiology, Reston, VA, 2013, ch. ACR BI-RADS Mammography.

[55] SIMONYAN, K., AND ZISSERMAN, A. Very deep convolutional networks for large-scale image recognition. *CoRR abs/1409.1556* (2014). Available online on `arxiv.org/abs/1409.1556`.

[56] SKAANE, P., HOFVIND, S., AND SKJENNALD, A. Randomized trial of screen-film versus full-field digital mammography with soft-copy reading in population-based screening program: Follow-up and final results of oslo II study. *Radiology 244*, 3 (2007), 708–717. PMID: 17709826.

[57] SPRINGENBERG, J. T., DOSOVITSKIY, A., BROX, T., AND RIEDMILLER, M. A. Striving for simplicity: The all convolutional net. *CoRR abs/1412.6806* (2014). Available online on `arxiv.org/abs/1412.6806`.

[58] SRIVASTAVA, N., HINTON, G., KRIZHEVSKY, A., SUTSKEVER, I., AND SALAKHUTDINOV, R. Dropout: A simple way to prevent neural networks from overfitting. *Journal of Machine Learning Research 15* (2014), 1929–1958.

[59] TAIGMAN, Y., YANG, M., RANZATO, M., AND WOLF, L. DeepFace: Closing the gap to human-level performance in face verification. In *Computer Vision and Pattern Recognition (CVPR)* (Columbus, Ohio, June 2014).

[60] TANG, J., RANGAYYAN, R., XU, J., EL NAQA, I., AND YANG, Y. Computer-aided detection and diagnosis of breast cancer with mammography: Recent advances. *Information Technology in Biomedicine, IEEE Transactions on 13*, 2 (March 2009), 236–251.

[61] WEI, D., SAHINER, B., CHAN, H.-P., AND PETRICK, N. Detection of masses on mammograms using a convolution neural network. In *International Conference on Acoustics, Speech, and Signal Processing, 1995. ICASSP-95.* (May 1995), vol. 5, pp. 3483–3486.

[62] WERBOS, P. J. *Beyond regression: new tools for prediction and analysis in the behavioral sciences*. PhD thesis, Harvard University, Boston, MA, 1974.

[63] WIDROW, B., AND HOFF, M. E. Adaptive switching circuits. In *1960 IRE WESCON Convention Record, Part 4* (New York, 1960), IRE, pp. 96–104.

Curriculum Vitae

Erick Michael Cobos Tandazo was born in Macará, Ecuador on March 10, 1992. He earned a B.S. Computer Science and Technology from the Instituto Tecnológico y de Estudios Superiores de Monterrey, Monterrey Campus in December 2014. He was accepted in the graduate program in Intelligent Systems in January 2015.

This document was typed in using LaTeX 2_ε[a] by Erick Michael Cobos Tandazo.

[a]The style file `thesisFormat.sty` used to set up this thesis was prepared by the Center of Intelligent Systems of the Instituto Tecnológico y de Estudios Superiores de Monterrey, Monterrey Campus